PHYSICAL REVIEW D **80,** 015013 (2009)

Intermediate mass scales in the nonsupersymmetric $SO(10)$ grand unification: A reappraisal

Stefano Bertolini* and Luca Di Luzio†
INFN, Sezione di Trieste, and SISSA, Via Beirut 4, I-34014 Trieste, Italy

Michal Malinský‡
Theoretical Particle Physics Group, Department of Theoretical Physics, Royal Technical Institute (KTH), Roslagstullsbacken 21, SE-106 91 Stockholm, Sweden

(Received 27 March 2009; published 17 July 2009)

The constraints of gauge unification on intermediate mass scales in nonsupersymmetric $SO(10)$ scenarios are systematically discussed. With respect to the existing reference studies we include the $U(1)$ gauge mixing renormalization at the one- and two-loop level, and reassess the two-loop beta coefficients. We evaluate the effects of additional Higgs multiplets required at intermediate stages by a realistic mass spectrum and update the discussion to the present day data. On the basis of the obtained results, $SO(10)$ breaking patterns with up to two intermediate mass scales are discussed for potential relevance and model predictivity.

DOI: 10.1103/PhysRevD.80.015013 PACS numbers: 12.10.Dm, 12.10.Kt, 11.10.Hi

I. INTRODUCTION

Understanding theoretically the patterns of masses and mixings of ordinary fermions is one of the long aimed goals in particle physics. Of the 56 parameters in the standard model (SM) Yukawa sector (including Majorana neutrinos) only 22 can be measured at low energy and just 17 have been determined from the experiment. Grand unified theories (GUTs), by enforcing stringent relations among the different particle sectors and by reducing the degeneracy in the parameter space, do provide a powerful tool for addressing the multiplicity of matter states and the detailed structure of the Yukawa sector.

Appealing candidates for realistic GUTs are models based on the $SO(10)$ gauge group [1]. All the known SM fermions plus three right-handed neutrinos fit into three copies of the 16-dimensional spinorial representation of $SO(10)$, thus providing a rationale for the SM hypercharge structure. The model also provides a natural explanation for the sub-eV light neutrino masses via the seesaw mechanism [2,3].

The purpose of this paper is to review the constraints enforced by gauge unification on the intermediate mass scales in the nonsupersymmetric $SO(10)$ GUTs, a needed preliminary step for assessing the structure of the multitude of the different breaking patterns before entering the details of a specific model. Eventually, our goal is to envisage and examine scenarios potentially relevant for the understanding of the low energy matter spectrum. In particular those setups that, albeit nonsupersymmetric, may exhibit a predictivity comparable to that of the minimal supersymmetric $SO(10)$, scrutinized at length in the last few years [4].

The most recent discussion of fermion masses and mixings in nonsupersymmetric $SO(10)$ GUTs was given in Ref. [5]. The authors focussed only on renormalizable models (i.e. without the spinorial $\overline{16}_H$ in the Higgs sector) with combinations of 10_H and $\overline{126}_H$ or 120_H driving the Yukawa interactions. Particular attention is paid to the leptonic sector and the mechanism of generation of neutrino masses via seesaw.

The constraints imposed by the absolute neutrino mass scale on the position of the $B - L$ threshold, together with the proton decay bound on the unification scale M_U, provide a discriminating tool among the many $SO(10)$ scenarios and the corresponding breaking patterns. These were studied at length in the eighties and early nineties, and detailed surveys of two- and three-step $SO(10)$ breaking chains (one and two intermediate thresholds, respectively) are found in Refs. [6–9].

We perform a systematic survey of $SO(10)$ unification with two intermediate stages. In addition to updating the analysis to present day data, this reappraisal is motivated by (a) the absence of $U(1)$ mixing in previous studies, both at one and two loops in the gauge coupling renormalization, (b) the need for additional Higgs multiplets at some intermediate stages, and (c) a reassessment of the two-loop beta coefficients reported in the literature.

The outcome of our study is the emergence of sizably different features in some of the breaking patterns as compared to the existing results. This allows us to rescue previously excluded scenarios. All that before considering the effects of threshold corrections [10–12], that are unambiguously assessed only when the details of a specific model are worked out.

It is remarkable that the chains corresponding to the minimal $SO(10)$ setup with the smallest Higgs representations (10_H, 45_H, and $\overline{16}_H$, or $\overline{126}_H$ in the renormalizable case) and the smallest number of parameters in the Higgs

*bertolin@sissa.it
†diluzio@sissa.it
‡malinsky@kth.se

potential, are still viable. The complexity of this nonsupersymmetric scenario is comparable to that of the minimal supersymmetric $SO(10)$ model, which makes it worth detailed consideration.

In Sec. II we set the framework of the analysis. Section III provides a collection of the tools needed for a two-loop study of grand unification. The results of the numerical study are reported and scrutinized in Sec. IV. Perspectives for further progress are discussed in Sec. V. Finally, the relevant one- and two-loop β coefficients are detailed in Appendix A.

II. THREE-STEP $SO(10)$ BREAKING CHAINS

The relevant $SO(10) \to G2 \to G1 \to \mathrm{SM}$ symmetry breaking chains with two intermediate gauge groups $G2$ and $G1$ are listed in Table I. Effective two-step chains are obtained by identifying two of the high-energy scales, paying attention to the possible deviations from minimality of the scalar content in the remaining intermediate stage (this we shall discuss in Sec. IV B).

For the purpose of comparison we follow closely the notation of Ref. [9], where P denotes the unbroken D parity [13]. For each step the Higgs representation responsible for the breaking is given.

The breakdown of the lower intermediate symmetry $G1$ to the SM gauge group is driven either by the 16- or 126-dimensional Higgs multiplets $\overline{16}_H$ or $\overline{126}_H$. An important feature of the scenarios with $\overline{126}_H$ is the fact that in such a case a potentially realistic $SO(10)$ Yukawa sector can be constructed already at the renormalizable level. Together with 10_H all the effective Dirac Yukawa couplings as well as the Majorana mass matrices at the SM level emerge from the contractions of the matter bilinears $16_F 16_F$ with $\overline{126}_H$ or with $\overline{16}_H \overline{16}_H/\Lambda$, where Λ denotes the scale (above M_U) at which the effective dimension five Yukawa couplings arise.

TABLE I. Relevant $SO(10)$ symmetry breaking chains via two intermediate gauge groups $G1$ and $G2$. For each step the representation of the Higgs multiplet (in $SO(10)$ notation) responsible for the breaking is given. The breaking to the SM group $1_Y 2_L 3_c$ is obtained via a 16 or 126 Higgs representation. The naming and ordering of the gauge groups follows the notation of Ref. [9].

Chain	$G2$	$G1$
I:	$\to_{210}\{2_L 2_R 4_C\}$	$\to_{45}\{2_L 2_R 1_X 3_c\}$
II:	$\to_{54}\{2_L 2_R 4_C P\}$	$\to_{210}\{2_L 2_R 1_X 3_c P\}$
III:	$\to_{54}\{2_L 2_R 4_C P\}$	$\to_{45}\{2_L 2_R 1_X 3_c\}$
IV:	$\to_{210}\{2_L 2_R 1_X 3_c P\}$	$\to_{45}\{2_L 2_R 1_X 3_c\}$
V:	$\to_{210}\{2_L 2_R 4_C\}$	$\to_{45}\{2_L 1_R 4_C\}$
VI:	$\to_{54}\{2_L 2_R 4_C P\}$	$\to_{45}\{2_L 1_R 4_C\}$
VII:	$\to_{54}\{2_L 2_R 4_C P\}$	$\to_{210}\{2_L 2_R 4_C\}$
VIII:	$\to_{45}\{2_L 2_R 1_X 3_c\}$	$\to_{45}\{2_L 1_R 1_X 3_c\}$
IX:	$\to_{210}\{2_L 2_R 1_X 3_c P\}$	$\to_{45}\{2_L 1_R 1_X 3_c\}$
X:	$\to_{210}\{2_L 2_R 4_C\}$	$\to_{210}\{2_L 1_R 1_X 3_c\}$
XI:	$\to_{54}\{2_L 2_R 4_C P\}$	$\to_{210}\{2_L 1_R 1_X 3_c\}$
XII:	$\to_{45}\{2_L 1_R 4_C\}$	$\to_{45}\{2_L 1_R 1_X 3_c\}$

The Higgs transforming as 10 under $SO(10)$ may carry in general extra quantum numbers of a complex representation of some additional symmetry (a discussion on the implementation of a Peccei-Quinn $U(1)_{PQ}$ symmetry in this scenario is given in Ref. [5]). In this case it is sufficient to consider only two complex symmetric matrices Y_{10} and Y_{126} at the renormalizable $SO(10)$ level, namely

$$16_F (Y_{10} 10_H + Y_{126} \overline{126}_H) 16_F, \tag{1}$$

that govern all the effective Yukawa couplings at lower energies. Such scenarios are rather constrained and hence their detailed numerical studies are well motivated.

D parity is a discrete symmetry acting as charge conjugation in a left-right symmetric context [13], and as that it plays the role of a left-right symmetry (it enforces for instance equal left and right gauge couplings). $SO(10)$ invariance then implies exact D parity (because D belongs to the $SO(10)$ Lie algebra). D parity may be spontaneously broken by D-odd Pati-Salam (PS) singlets contained in 210 or 45 Higgs representations. Its breaking can therefore be decoupled from the $SU(2)_R$ breaking, allowing for different left and right gauge couplings.

The possibility of decoupling the D-parity breaking from the scale of right-handed interactions is a cosmologically relevant issue. On the one hand, baryon asymmetry cannot arise in a left-right symmetric ($g_L = g_R$) universe [14]. On the other hand, the spontaneous breaking of a discrete symmetry, such as D parity, creates domain walls that, if massive enough (i.e. for intermediate mass scales) do not disappear, overclosing the universe [15]. These potential problems may be overcome either by confining D parity at the GUT scale or by invoking inflation. The latter solution implies that domain walls are formed above the reheating temperature, enforcing a lower bound on the D-parity breaking scale of 10^{12} GeV. Realistic $SO(10)$ breaking patterns must therefore include this constraint.

A. The extended survival hypothesis

Throughout all three stages of running we assume that the scalar spectrum obeys the so-called extended survival hypothesis (ESH) [16] which requires that *at every stage of the symmetry breaking chain only those scalars are present that develop a vacuum expectation value (VEV) at the current or the subsequent levels of the spontaneous symmetry breaking*. ESH is equivalent to the requirement of the minimal number of fine-tunings to be imposed onto the scalar potential [17] so that all the symmetry breaking steps are performed at the desired scales.

On the technical side one should identify all the Higgs multiplets needed by the breaking pattern under consideration and keep them according to the gauge symmetry down to the scale of their VEVs. This typically pulls down a large

number of scalars in scenarios where $\overline{126}_H$ provides the $B-L$ breakdown.

On the other hand, one must take into account that the role of $\overline{126}_H$ is twofold: in addition to triggering the $G1$ breaking it plays a relevant role in the Yukawa sector (Eq. (1)) where it provides the necessary breaking of the down quark-charged lepton mass degeneracy. For this to work one needs a reasonably large admixture of the $\overline{126}_H$ component in the effective electroweak doublets. Since $(2,2,1)_{10}$ can mix with $(2,2,15)_{\overline{126}}$ only below the Pati-Salam breaking scale, both fields must be present at the Pati-Salam level (otherwise the scalar doublet mass matrix does not provide large enough components of both these multiplets in the light Higgs fields).

Note that the same argument applies also to the $2_L1_R4_C$ intermediate stage when one must retain the doublet component of $\overline{126}_H$, namely $(2,+\frac{1}{2},15)_{\overline{126}}$, in order for it to eventually admix with $(2,+\frac{1}{2},1)_{10}$ in the light Higgs sector. On the other hand, at the $2_L2_R1_X3_c$ and $2_L1_R1_X3_c$ stages, the (minimal) survival of only one combination of the ϕ^{10} and ϕ^{126} scalar doublets (see Table II) is compatible with the Yukawa sector constraints because the degeneracy between the quark and lepton spectra has already been smeared out by the Pati-Salam breakdown.

In summary, potentially realistic renormalizable Yukawa textures in settings with well-separated $SO(10)$ and Pati-Salam breaking scales call for an additional fine-tuning in the Higgs sector. In the scenarios with $\overline{126}_H$, the 10_H bidoublet $(2,2,1)_{10}$, included in Refs [6–9], must be paired at the $2_L2_R4_C$ scale with an extra $(2,2,15)_{\overline{126}}$ scalar bidoublet (or $(2,+\frac{1}{2},1)_{10}$ with $(2,+\frac{1}{2},15)_{\overline{126}}$ at the $2_L1_R4_C$ stage). This can affect the running of the gauge couplings in chains I, II, III, V, VI, VII, X, XI, and XII.

For the sake of comparison with previous studies [6–9] we shall not include the ϕ^{126} multiplets in the first part of the analysis. Rather, we shall comment on their relevance for gauge unification in Sec. IV C.

TABLE II. Scalar multiplets contributing to the running of the gauge couplings for a given $SO(10)$ subgroup according to minimal fine-tuning. The survival of ϕ^{126} (not required by minimality) is needed by a realistic leptonic mass spectrum, as discussed in the text (in the $2_L2_R1_X3_c$ and $2_L1_R1_X3_c$ stages only one linear combination of ϕ^{10} and ϕ^{126} remains). The $U(1)_X$ charge is given, up to a factor $\sqrt{3/2}$, by $(B-L)/2$ (the latter is reported in the table). For the naming of the Higgs multiplets we follow the notation of Ref. [9] with the addition of ϕ^{126}. When the D parity (P) is unbroken the particle content must be left-right symmetric. D parity may be broken via P-odd Pati-Salam singlets in 45_H or 210_H.

Surviving Higgs multiplets in $SO(10)$ subgroups					
$SO(10)$	$\{2_L1_R4_C\}$	$\{2_L2_R4_C\}$	$\{2_L2_R1_X3_{c'}\}$	$\{2_L1_R1_X3_{c'}\}$	Notation
10	$(2,+\frac{1}{2},1)$	$(2,2,1)$	$(2,2,0,1)$	$(2,+\frac{1}{2},0,1)$	ϕ^{10}
$\overline{16}$	$(1,+\frac{1}{2},4)$	$(1,2,4)$	$(1,2,-\frac{1}{2},1)$	$(1,+\frac{1}{2},-\frac{1}{2},1)$	δ_R^{16}
$\overline{16}$		$(2,1,\bar{4})$	$(2,1,+\frac{1}{2},1)$		δ_L^{16}
$\overline{126}$	$(2,+\frac{1}{2},15)$	$(2,2,15)$	$(2,2,0,1)$	$(2,+\frac{1}{2},0,1)$	ϕ^{126}
$\overline{126}$	$(1,1,10)$	$(1,3,10)$	$(1,3,-1,1)$	$(1,1,-1,1)$	Δ_R^{126}
$\overline{126}$		$(3,1,\overline{10})$	$(3,1,1,1)$		Δ_L^{126}
45	$(1,0,15)$	$(1,1,15)$			Λ^{45}
210		$(1,1,15)$			Λ^{210}
45		$(1,3,1)$	$(1,3,0,1)$		Σ_R^{45}
45		$(3,1,1)$	$(3,1,0,1)$		Σ_L^{45}
210		$(1,3,15)$			σ_R^{210}
210		$(3,1,15)$			σ_L^{210}

III. TWO-LOOP GAUGE RENORMALIZATION GROUP EQUATIONS

In this section we report, in order to fix a consistent notation, the two-loop renormalization group equations (RGEs) for the gauge couplings. We consider a gauge group of the form $U(1)_1\otimes\ldots\otimes U(1)_N\otimes G_1\otimes\ldots\otimes G_{N'}$, where G_i are simple groups.

A. The non-Abelian sector

Let us focus first on the non-Abelian sector corresponding to $G_1\otimes\ldots\otimes G_{N'}$ and defer the full treatment of the effects due to the extra $U(1)$ factors to Sec. III B. Defining $t=\log(\mu/\mu_0)$ we write

$$\frac{dg_p}{dt}=g_p\beta_p, \tag{2}$$

where $p=1,\ldots,N'$ is the gauge group label. Neglecting for the time being the Abelian components, the β functions for the $G_1\otimes\ldots\otimes G_{N'}$ gauge couplings read at two-loop level [18–21]:

$$\begin{aligned}\beta_p=&\frac{g_p^2}{(4\pi)^2}\Big\{-\frac{11}{3}C_2(G_p)+\frac{4}{3}\kappa S_2(F_p)+\frac{1}{3}\eta S_2(S_p)\\&-\frac{2\kappa}{(4\pi)^2}Y_4(F_p)+\frac{g_p^2}{(4\pi)^2}\Big[-\frac{34}{3}(C_2(G_p))^2\\&+\Big(4C_2(F_p)+\frac{20}{3}C_2(G_p)\Big)\kappa S_2(F_p)\\&+\Big(4C_2(S_p)+\frac{2}{3}C_2(G_p)\Big)\eta S_2(S_p)\Big]\\&+\frac{g_q^2}{(4\pi)^2}4[\kappa C_2(F_q)S_2(F_p)+\eta C_2(S_q)S_2(S_p)]\Big\},\end{aligned} \tag{3}$$

where $\kappa=1,\frac{1}{2}$ for Dirac and Weyl fermions, respectively. Correspondingly, $\eta=1,\frac{1}{2}$ for complex and real scalar fields. The sum over $q\neq p$ corresponding to contributions to β_p from the other gauge sectors labeled by q is understood. Given a fermion F or a scalar S field that transforms according to the representation $R=R_1\otimes\ldots\otimes R_{N'}$, where R_p is an irreducible representation of the group G_p of dimension $d(R_p)$, the factor $S_2(R_p)$ is defined by

$$S_2(R_p) \equiv T(R_p)\frac{d(R)}{d(R_p)}, \tag{4}$$

where $T(R_p)$ is the Dynkin index of the representation R_p. The corresponding Casimir eigenvalue is then given by

$$C_2(R_p)d(R_p) = T(R_p)d(G_p), \tag{5}$$

where $d(G)$ is the dimension of the group. In Eq. (3) the first row represents the one-loop contribution while the other terms stand for the two-loop corrections, including that induced by Yukawa interactions. The latter is accounted for in terms of a factor

$$Y_4(F_p) = \frac{1}{d(G_p)}\,\mathrm{Tr}[C_2(F_p)YY^\dagger], \tag{6}$$

where the ''general'' Yukawa coupling

$$Y^{abc}\bar{\psi}_a\psi_b h_c + \mathrm{H.c.} \tag{7}$$

includes family as well as group indices. The coupling in Eq. (7) is written in terms of four-component Weyl spinors $\psi_{a,b}$ and a scalar field h_c (be complex or real). The trace includes the sum over all relevant fermion and scalar fields.

B. The Abelian couplings and $U(1)$ mixing

In order to include the Abelian contributions to Eq. (3) at two loops and the one- and two-loop effects of $U(1)$ mixing [22], let us write the most general interaction of N Abelian gauge bosons A_b^μ and a set of Weyl fermions ψ_f as

$$\bar{\psi}_f\gamma_\mu Q_f^r\psi_f g_{rb}A_b^\mu. \tag{8}$$

The gauge coupling constants g_{rb}, $r, b = 1, \ldots, N$, couple A_b^μ to the fermionic current $J_\mu^r = \bar{\psi}_f\gamma_\mu Q_f^r\psi_f$. The $N \times N$ gauge coupling matrix g_{rb} can be diagonalized by two independent rotations: one acting on the $U(1)$ charges Q_f^r and the other on the gauge-boson fields A_b^μ. For a given choice of the charges, g_{rb} can be set in a triangular form ($g_{rb} = 0$ for $r > b$) by the gauge-boson rotation. The resulting $N(N+1)/2$ entries are observable couplings.

Since $F_{\mu\nu}^a$ in the Abelian case is itself gauge invariant, the most general kinetic part of the Lagrangian reads at the renormalizable level

$$-\tfrac{1}{4}F_{\mu\nu}^a F^{a\mu\nu} - \tfrac{1}{4}\xi_{ab}F_{\mu\nu}^a F^{b\mu\nu}, \tag{9}$$

where $a \neq b$ and $|\xi_{ab}| < 1$. A nonorthogonal rotation of the fields A_a^μ may be performed to set the gauge kinetic term in a canonical diagonal form. Any further orthogonal rotation of the gauge fields will preserve this form. Then, the renormalization prescription may be conveniently chosen to maintain at each scale the kinetic terms canonical and diagonal on shell while renormalizing accordingly the gauge coupling matrix g_{rb}.[1] Thus, even if at one scale g_{rb} is diagonal, in general nonzero off-diagonal entries are generated by renormalization effects. One shows [24] that in the case the Abelian gauge couplings are at a given scale diagonal *and* equal (i.e. there is a $U(1)$ unification), there may exist a (scale independent) gauge field basis such that the Abelian interactions remain to all orders diagonal along the RGE trajectory.[2]

In general, the renormalization of the Abelian part of the gauge interactions is determined by

$$\frac{dg_{rb}}{dt} = g_{ra}\beta_{ab}, \tag{10}$$

where, as a consequence of gauge invariance,

$$\beta_{ab} = \frac{d}{dt}(\log Z_3^{1/2})_{ab} \tag{11}$$

with Z_3 denoting the gauge-boson wave-function renormalization matrix. In order to further simplify the notation it is convenient to introduce the ''reduced'' couplings [24]

$$g_{kb} \equiv Q_k^r g_{rb}, \tag{12}$$

that evolve according to

$$\frac{dg_{kb}}{dt} = g_{ka}\beta_{ab}. \tag{13}$$

The index k labels the fields (fermions and scalars) that carry $U(1)$ charges.

In terms of the reduced couplings the β function that governs the $U(1)$ running up to two loops is given by [18–20]

$$\begin{aligned}\beta_{ab} = \frac{1}{(4\pi)^2}\Big\{&\frac{4}{3}\kappa g_{fa}g_{fb} + \frac{1}{3}\eta g_{sa}g_{sb} \\ &- \frac{2\kappa}{(4\pi)^2}\,\mathrm{Tr}[g_{fa}g_{fb}YY^\dagger] \\ &+ \frac{4}{(4\pi)^2}[\kappa(g_{fa}g_{fb}g_{fc}^2 + g_{fa}g_{fb}g_q^2C_2(F_q)) \\ &+ \eta(g_{sa}g_{sb}g_{sc}^2 + g_{sa}g_{sb}g_q^2C_2(S_q))]\Big\},\end{aligned} \tag{14}$$

where repeated indices are summed over, labeling fermions (f), scalars (s), and $U(1)$ gauge groups (c). The terms proportional to the quadratic Casimir $C_2(R_p)$ represent the two-loop contributions of the non-Abelian components G_q of the gauge group to the $U(1)$ gauge coupling renormalization.

Correspondingly, using the notation of Eq. (12), an additional two-loop term that represents the renormalization of the non-Abelian gauge couplings induced at two loops by the $U(1)$ gauge fields is to be added to Eq. (3), namely

[1] Alternatively one may work with off-diagonal kinetic terms while keeping the gauge interactions diagonal [23].

[2] Vanishing of the commutator of the β functions and their derivatives is needed [25].

$$\Delta\beta_p = \frac{g_p^2}{(4\pi)^4} 4[\kappa g_{fc}^2 S_2(F_p) + \eta g_{sc}^2 S_2(S_p)]. \quad (15)$$

In Eqs. (14) and (15), we use the abbreviation $f \equiv F_p$ and $s \equiv S_p$ and, as before, $\kappa = 1, \frac{1}{2}$ for Dirac and Weyl fermions, while $\eta = 1, \frac{1}{2}$ for complex and real scalar fields, respectively.

C. Some notation

When at most one $U(1)$ factor is present, and neglecting the Yukawa contributions, the two-loop RGEs can be conveniently written as

$$\frac{d\alpha_i^{-1}}{dt} = -\frac{a_i}{2\pi} - \frac{b_{ij}}{8\pi^2}\alpha_j, \quad (16)$$

where $\alpha_i = g_i^2/4\pi$. The β coefficients a_i and b_{ij} for the relevant $SO(10)$ chains are given in Appendix A.

Substituting the one-loop solution for α_j into the right-hand side (RHS) of Eq. (16) one obtains

$$\alpha_i^{-1}(t) - \alpha_i^{-1}(0) = -\frac{a_i}{2\pi}t + \frac{\tilde{b}_{ij}}{4\pi}\log(1-\omega_j t), \quad (17)$$

where $\omega_j = a_j\alpha_j(0)/(2\pi)$ and $\tilde{b}_{ij} = b_{ij}/a_j$. The analytic solution in (17) holds at two loops (for $\omega_j t < 1$) up to higher order effects. A sample of the rescaled β coefficients $\tilde{b}_{ij}$ is given, for the purpose of comparison with previous results, in Appendix A.

We shall conveniently write the β function in Eq. (14), that governs the Abelian mixing, as

$$\beta_{ab} = \frac{1}{(4\pi)^2} g_{sa}\gamma_{sr}g_{rb}, \quad (18)$$

where γ_{sr} include both one- and two-loop contributions. Analogously, the non-Abelian beta function in Eq. (3), including the $U(1)$ contribution in Eq. (15), is conveniently written as

$$\beta_p = \frac{g_p^2}{(4\pi)^2}\gamma_p. \quad (19)$$

The γ_p functions for the $SO(10)$ breaking chains considered in this work are reported in Appendix A 1.

Finally, the Yukawa term in Eq. (6), and correspondingly in Eq. (14), can be written as

$$Y_4(F_p) = y_{pk}\,\mathrm{Tr}(Y_k Y_k^\dagger), \quad (20)$$

where Y_k are the "standard" 3×3 Yukawa matrices in the family space labeled by the flavor index k. The trace is taken over family indices and k is summed over the different Yukawa terms present at each stage of $SO(10)$ breaking. The coefficients y_{pk} are given explicitly in Appendix A.

D. One-loop matching

The matching conditions between effective theories in the framework of dimensional regularization have been derived in [26,27]. Let us consider first a simple gauge group G spontaneously broken into subgroups G_p. Neglecting terms involving logarithms of mass ratios which are expected to be subleading (massive states clustered near the threshold[3]) the one-loop matching for the gauge couplings can be written as

$$\alpha_p^{-1} - \frac{C_2(G_p)}{12\pi} = \alpha_G^{-1} - \frac{C_2(G)}{12\pi}. \quad (21)$$

Let us turn to the case when several non-Abelian simple groups G_p (and at most one $U(1)_X$) spontaneously break while preserving a $U(1)_Y$ charge. The conserved $U(1)$ generator T_Y can be written in terms of the relevant generators of the various Cartan subalgebras (and of the consistently normalized T_X) as

$$T_Y = p_i T_i, \quad (22)$$

where $\sum p_i^2 = 1$, and i runs over the relevant p (and X) indices. The matching condition is then given by

$$\alpha_Y^{-1} = \sum_i p_i^2\left(\alpha_i^{-1} - \frac{C_2(G_i)}{12\pi}\right), \quad (23)$$

where for $i = X$, if present, $C_2 = 0$.

Consider now the breaking of N copies of $U(1)$ gauge factors to a subset of M elements $U(1)$ (with $M < N$). Denoting by T_n $(n = 1, \ldots, N)$ and by $\tilde{T}_m$ $(m = 1, \ldots, M)$ their properly normalized generators we have

$$\tilde{T}_m = P_{mn}T_n \quad (24)$$

with the orthogonality condition $P_{mn}P_{m'n} = \delta_{mm'}$. Let us denote by g_{na} $(n,\ a = 1, \ldots, N)$ and by $\tilde{g}_{mb}$ $(m,\ b = 1, \ldots, M)$ the matrices of Abelian gauge couplings above and below the breaking scale, respectively. By writing the Abelian gauge-boson mass matrix in the broken vacuum and by identifying the massless states, we find the following matching condition:

$$(\tilde{g}\tilde{g}^T)^{-1} = P(gg^T)^{-1}P^T. \quad (25)$$

Notice that Eq. (25) depends on the chosen basis for the $U(1)$ charges (via P) but it is invariant under orthogonal rotations of the gauge-boson fields ($gO^T Og^T = gg^T$). The massless gauge bosons $\tilde{A}_m^\mu$ are given in terms of A_n^μ by

$$\tilde{A}_m^\mu = [\tilde{g}^T P(g^{-1})^T]_{mn}A_n^\mu, \quad (26)$$

where $m = 1, \ldots, M$ and $n = 1, \ldots, N$.

The general case of a gauge group $U(1)_1 \otimes \ldots \otimes U(1)_N \otimes G_1 \otimes \ldots \otimes G_{N'}$ spontaneously broken to $U(1)_1 \otimes \ldots \otimes U(1)_M$ with $M \leq N + N'$ is taken care of by replac-

[3] An early discussion of thresholds effects in $SO(10)$ GUT is found in [10].

ing $(gg^T)^{-1}$ in Eq. (25) with the block-diagonal $(N + N') \times (N + N')$ matrix

$$(GG^T)^{-1} = \mathrm{Diag}\left[(gg^T)^{-1}, g_p^{-2} - \frac{C_2(G_p)}{48\pi^2}\right] \tag{27}$$

thus providing, together with the extended Eqs. (24) and (25), a generalization of Eq. (23).

IV. NUMERICAL RESULTS

At one loop, and in the absence of the $U(1)$ mixing, the gauge RGEs are not coupled and the unification constraints can be studied analytically. When two-loop effects are included (or at one loop more than one $U(1)$ factor is present) there is no closed solution and one must solve the system of coupled equations, matching all stages between the weak and unification scales, numerically. On the other hand (when no $U(1)$ mixing is there) one may take advantage of the analytic formula in Eq. (17). The latter turns out to provide, for the cases here studied, a very good approximation to the numerical solution. The discrepancies with the numerical integration do not generally exceed the 10^{-3} level.

We perform a scan over the relevant breaking scales M_U, M_2, and M_1 and the value of the grand unified coupling α_U and impose the matching with the SM gauge couplings at the M_Z scale requiring a precision at the per-mil level. This is achieved by minimizing the parameter

$$\delta = \sqrt{\sum_{i=1}^{3}\left(\frac{\alpha_i^{\mathrm{th}} - \alpha_i}{\alpha_i}\right)^2}, \tag{28}$$

where α_is denote the experimental values at M_Z and α_i^{th} are the renormalized couplings obtained from unification.

The input values for the (consistently normalized) gauge SM couplings at the scale $M_Z = 91.19$ GeV are [28]

$$\begin{aligned} \alpha_1 &= 0.016\,946 \pm 0.000\,006, \\ \alpha_2 &= 0.033\,812 \pm 0.000\,021, \\ \alpha_3 &= 0.1176 \pm 0.0020, \end{aligned} \tag{29}$$

corresponding to the electroweak scale parameters

$$\begin{aligned} \alpha_{em}^{-1} &= 127.925 \pm 0.016, \\ \sin^2\theta_W &= 0.231\,19 \pm 0.000\,14. \end{aligned} \tag{30}$$

All these data refer to the modified minimally subtracted ($\overline{\mathrm{MS}}$) quantities at the M_Z scale.

For $\alpha_{1,2}$ we shall consider only the central values while we resort to scanning over the whole 3σ domain for α_3 when a stable solution is not found.

The results, i.e. the positions of the intermediate scales M_1, M_2, and M_U shall be reported in terms of decadic logarithms of their values in units of GeV, i.e. $n_1 = \log_{10}(M_1/\mathrm{GeV})$, $n_2 = \log_{10}(M_2/\mathrm{GeV})$, $n_U = \log_{10}(M_U/\mathrm{GeV})$. In particular, n_U, n_2 are given as functions of n_1 for each breaking pattern and for different approximations in the loop expansion. Each of the breaking patterns is further supplemented by the relevant range of the values of α_U.

A. $U(1)_R \times U(1)_X$ mixing

The chains VIII to XII require consideration of the mixing between the two $U(1)$ factors. While $U(1)_R$ and $U(1)_X$ do emerge with canonical diagonal kinetic terms, being the remnants of the breaking of non-Abelian groups, the corresponding gauge couplings are at the onset different in size. In general, no *scale-independent* orthogonal rotations of charges and gauge fields exist that diagonalize the gauge interactions to all orders along the RGE trajectories. According to the discussion in Sec. III, off-diagonal gauge couplings arise at the one-loop level that must be accounted for in order to perform the matching at the M_1 scale with the standard hypercharge. The preserved direction in the $Q^{R,X}$ charge space is given by

$$Q^Y = \sqrt{\tfrac{3}{5}}Q^R + \sqrt{\tfrac{2}{5}}Q^X, \tag{31}$$

where

$$Q^R = I_{3R} \quad \text{and} \quad Q^X = \sqrt{\frac{3}{2}}\left(\frac{B-L}{2}\right). \tag{32}$$

The matching of the gauge couplings is then obtained from Eq. (25)

$$g_Y^{-2} = P(gg^T)^{-1}P^T, \tag{33}$$

with

$$P = \left(\sqrt{\tfrac{3}{5}}, \sqrt{\tfrac{2}{5}}\right) \tag{34}$$

and

$$g = \begin{pmatrix} g_{RR} & g_{RX} \\ g_{XR} & g_{XX} \end{pmatrix}. \tag{35}$$

When neglecting the off-diagonal terms, Eq. (33) reproduces the matching condition used in Refs. [6–9]. For all other cases, in which only one $U(1)$ factor is present, the matching relations can be read off directly from Eqs. (21) and (23).

B. Two-loop results (purely gauge)

The results of the numerical analysis are organized as follows: Figs. 1 and 2 show the values of n_U and n_2 as functions of n_1 for the pure gauge running (i.e. no Yukawa interactions), in the $\overline{126}_H$ and $\overline{16}_H$ case, respectively. The differences between the patterns for the $\overline{126}_H$ and $\overline{16}_H$ setups depend on the substantially different scalar content. The shape and size of the various contributions (one loop, with and without $U(1)$ mixing, and two loops) are compared in each figure. The dissection of the RGE results shown in the figures allows us to compare our results with those of Refs. [6–9].

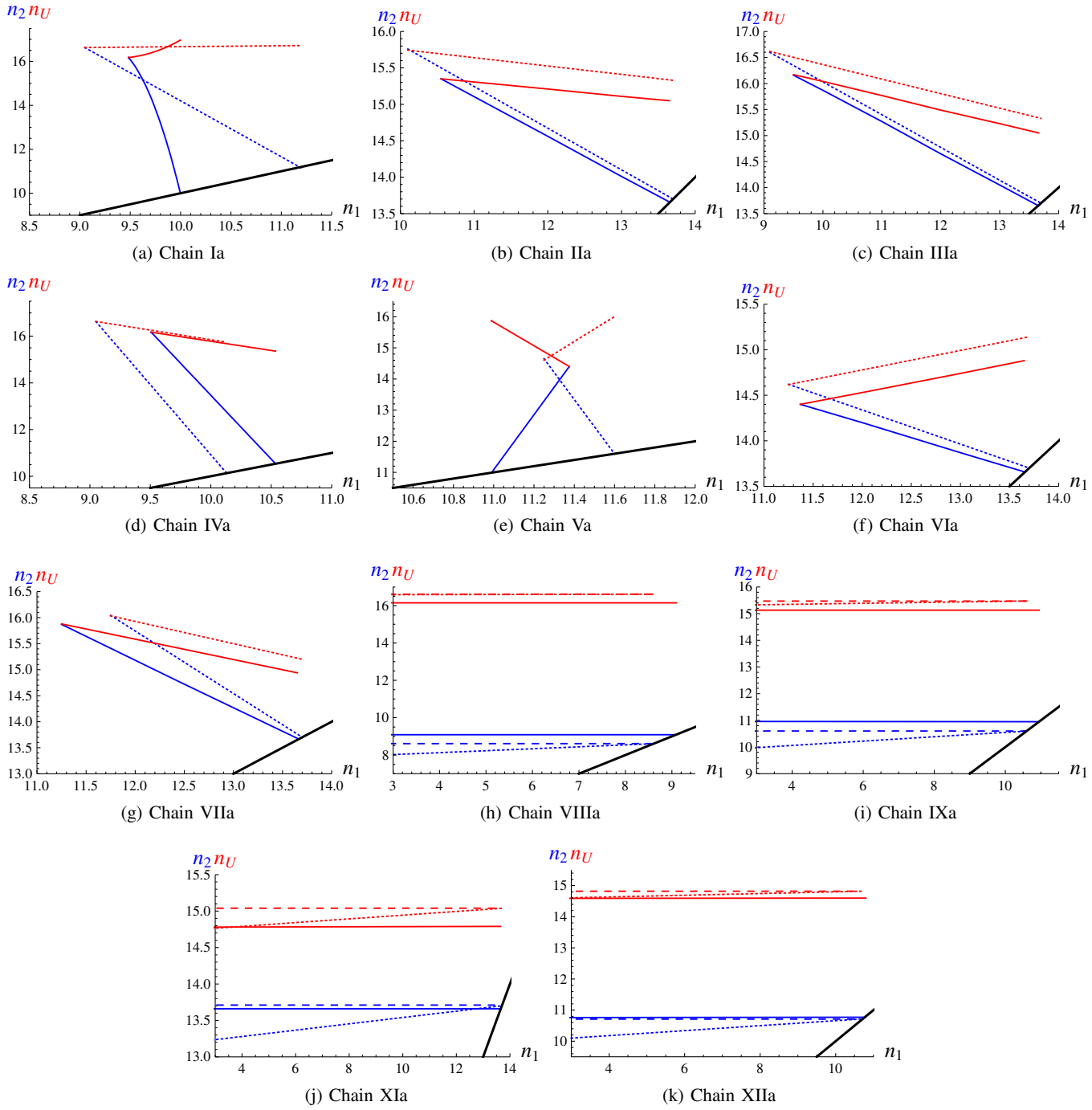

(a) Chain Ia (b) Chain IIa (c) Chain IIIa

(d) Chain IVa (e) Chain Va (f) Chain VIa

(g) Chain VIIa (h) Chain VIIIa (i) Chain IXa

(j) Chain XIa (k) Chain XIIa

FIG. 1 (color online). The values of n_U (red/upper branches) and n_2 (blue/lower branches) are shown as functions of n_1 for the pure gauge running in the $\overline{126}_H$ case. The bold black line bounds the region $n_1 \leq n_2$. From chains Ia to VIIa the short-dashed lines represent the result of one-loop running while the solid ones correspond to the two-loop solutions. For chains VIIIa to XIIa the short-dashed lines represent the one-loop results without the $U(1)_X \otimes U(1)_R$ mixing, the long-dashed lines account for the complete one-loop results, while the solid lines represent the two-loop solutions. The scalar content at each stage corresponds to that considered in Ref. [9], namely, to that reported in Table II without the ϕ^{126} multiplets. For chains I to VII the two-step $SO(10)$ breaking consistent with minimal fine-tuning is recovered in the $n_2 \to n_U$ limit. No solution is found for chain Xa.

Table III shows the two-loop values of α_U^{-1} in the allowed region for n_1. The contributions of the additional ϕ^{126} multiplets and the Yukawa terms are discussed separately in Secs. IV C and IV D, respectively. With the exception of a few singular cases detailed therein, these effects turn out to be generally subdominant.

As already mentioned in the introduction, two-loop precision in a GUT scenario makes sense once (one-

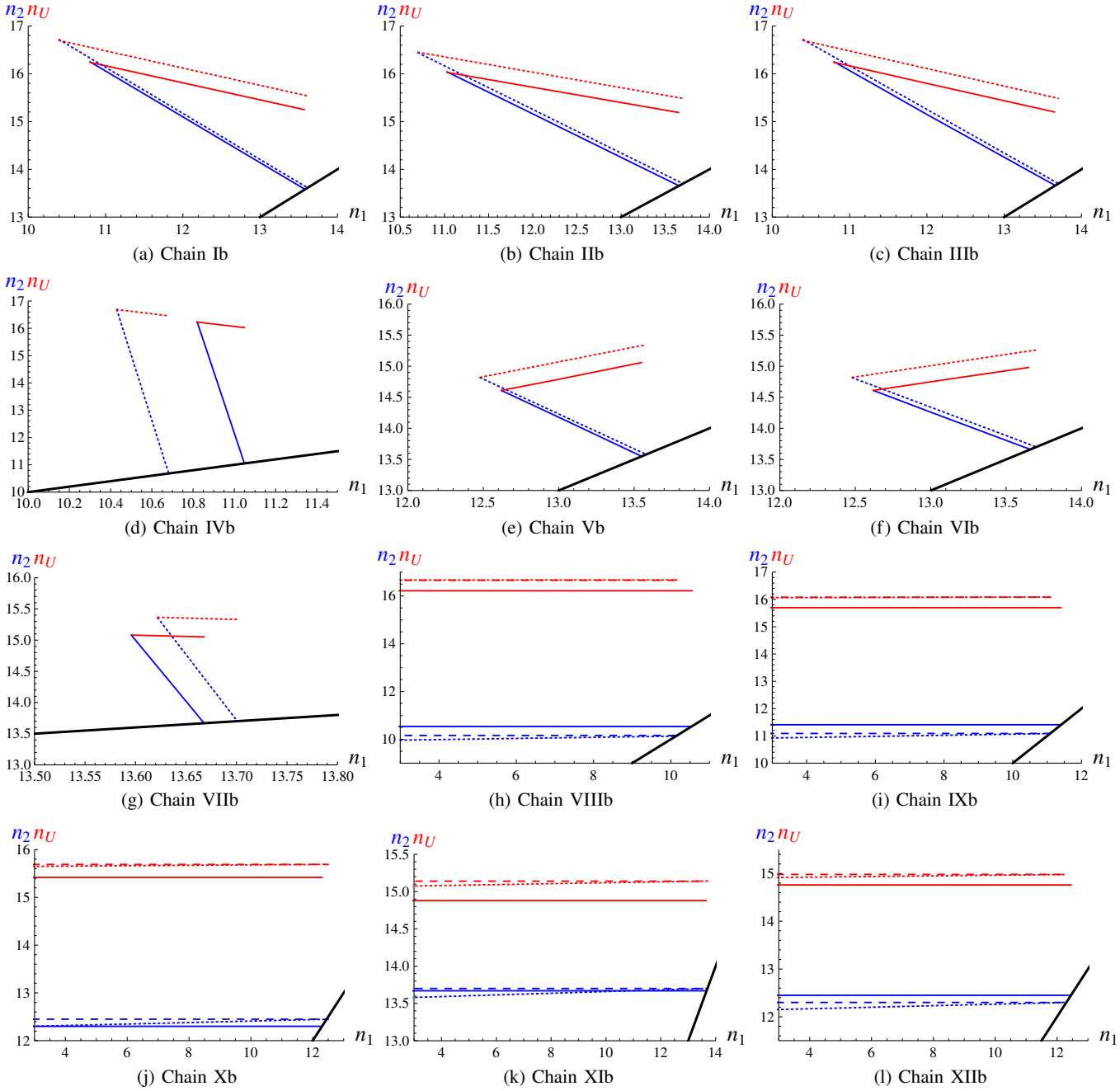

FIG. 2 (color online). Same as in Fig. 1 for the $\overline{16}_H$ case.

loop) thresholds effects are coherently taken into account, as their effect may become comparable if not larger than the two loop itself (the argument becomes stronger as the number of intermediate scales increases). On the other hand, there is no control on the spectrum unless a specific model is studied in detail. The purpose of this work is to set the stage for such a study by reassessing and updating the general constraints and patterns that $SO(10)$ grand unification enforces on the spread of intermediate scales.

The one and two-loop β coefficients used in the present study are reported in Appendix A. Table IX in the appendix shows the reduced $\tilde{b}_{ij}$ coefficients for those cases where we are at variance with Ref. [7].

One of the largest effects in the comparison with Refs. [6–9] emerges at one loop and it is due to the implementation of the $U(1)$ gauge mixing when $U(1)_R \otimes U(1)_X$ appears as an intermediate stage of the $SO(10)$ breaking.[4] This affects chains VIII to XII, and it exhibits

[4]The lack of Abelian gauge mixing in Ref. [9] was first observed in Ref. [29].

TABLE III. Two-loop values of α_U^{-1} in the allowed region for n_1. From chains I to VII, α_U^{-1} is n_1 dependent and its range is given in square brackets for the minimum (left) and the maximum (right) value of n_1, respectively. For chains VIII to XII, α_U^{-1} depends very weakly on n_1 (see the discussion on $U(1)$ mixing in the text). No solution is found for chain Xa.

Chain	α_U^{-1}	Chain	α_U^{-1}
Ia	[45.5, 46.4]	Ib	[45.7, 44.8]
IIa	[43.7, 40.8]	IIb	[45.3, 44.5]
IIIa	[45.5, 40.8]	IIIb	[45.7, 44.5]
IVa	[45.5, 43.4]	IVb	[45.7, 45.1]
Va	[45.4, 44.1]	Vb	[44.3, 44.8]
VIa	[44.1, 41.0]	VIb	[44.3, 44.2]
VIIa	[45.4, 41.1]	VIIb	[44.8, 44.4]
VIIIa	45.4	VIIIb	45.6
IXa	42.8	IXb	44.3
Xa		Xb	44.8
XIa	38.7	XIb	41.5
XIIa	44.1	XIIb	44.3

itself in the exact (one-loop) flatness of n_2, n_U, and α_U as functions of n_1.

The rationale for such a behavior is quite simple. When considering the gauge coupling renormalization in the $2_L 1_R 1_X 3_c$ stage, no effect at one loop appears in the non-Abelian β functions due to the Abelian gauge fields. On the other hand, the Higgs fields surviving at the $2_L 1_R 1_X 3_c$ stage, responsible for the breaking to $1_Y 2_L 3_c$, are (by construction) SM singlets. Since the SM one-loop β functions are not affected by their presence, the solution found for n_2, n_U, and α_U in the $n_1 = n_2$ case holds for $n_1 < n_2$ as well. Only by performing correctly the mixed $1_R 1_X$ gauge running and the consistent matching with 1_Y one recovers the expected n_1 flatness of the GUT solution.

In this respect, it is interesting to notice that the absence of $U(1)$ mixing in Refs. [6–9] makes the argument for the actual possibility of a light (observable) $U(1)_R$ gauge boson an ''approximate'' statement (based on the approximate flatness of the solution).

One expects this feature to break at two loops. The $SU(2)_L$ and $SU(3)_c$ β functions are affected at two loops directly by the Abelian gauge bosons via Eq. (15) (the Higgs multiplets that are responsible for the $U(1)_R \otimes U(1)_X$ breaking do not enter through the Yukawa interactions). The net effect on the non-Abelian gauge running is related to the difference between the contribution of the $U(1)_R$ and $U(1)_X$ gauge bosons and that of the standard hypercharge. We checked that such a difference is always a small fraction (below 10%) of the typical two-loop contributions to the $SU(2)_L$ and $SU(3)_c$ β functions. As a consequence, the n_1 flatness of the GUT solution is at a very high accuracy (10^{-3}) preserved at two loops as well, as the inspection of the relevant chains in Figs. 1 and 2 shows.

Still at one loop we find a sharp disagreement in the n_1 range of chain XIIa, with respect to the result of Ref. [9]. The authors find $n_1 < 5.3$, while strictly following their procedure and assumptions we find $n_1 < 10.2$ (the updated one- and two-loop results are given in Fig. 1(k)]. As we shall see, this difference brings chain XIIa back among the potentially realistic ones.

As far as two-loop effects are at stakes, their relevance is generally related to the length of the running involving the largest non-Abelian groups. On the other hand, there are chains where n_2 and n_U have a strong dependence on n_1 (we will refer to them as ''unstable'' chains) and where two-loop corrections affect substantially the one-loop results. Evident examples of such unstable chains are Ia, IVa, Va, IVb, and VIIb. In particular, in chain Va the two-loop effects flip the slopes of n_2 and n_U, that implies a sharp change in the allowed region for n_1. It is clear that when dealing with these breaking chains any statement about their viability should account for the details of the thresholds in the given model.

In chains VIII to XII (where the second intermediate stage is $2_L 1_R 1_X 3_c$, two-loop effects are mild and exhibit the common behavior of lowering the GUT scale (n_U) while raising (with the exception of Xb and XIa,b) the largest intermediate scale (n_2). The mildness of two-loop corrections (no more that one would *a priori* expect) is strictly related to the (n_1) flatness of the GUT solution discussed before.

Worth mentioning are the limits $n_2 \sim n_U$ and $n_1 \sim n_2$. While the former is equivalent to neglecting the first stage $G2$ and to reducing effectively the three breaking steps to just two (namely $SO(10) \rightarrow G1 \rightarrow \mathrm{SM}$) with a minimal fine-tuning in the scalar sector, care must be taken of the latter. One may naively expect that the chains with the same $G2$ should exhibit for $n_1 \sim n_2$ the same numerical behavior ($SO(10) \rightarrow G2 \rightarrow \mathrm{SM}$), thus clustering the chains (I,V,X), (II,III,VI,VII,XI), and (IV,IX). On the other hand, one must recall that the existence of $G1$ and its breaking remain encoded in the $G2$ stage through the Higgs scalars that are responsible for the $G2 \rightarrow G1$ breaking. This is why the chains with the same $G2$ are not in general equivalent in the $n_1 \sim n_2$ limit. The numerical features of the degenerate patterns (with $n_2 \sim n_U$) can be cross-checked among the different chains by direct inspection of Figs. 1 and 2 and Table III.

In any discussion of viability of the various scenarios the main attention is paid to the constraints emerging from the proton decay. In nonsupersymmetric GUTs, this process is mediated by baryon number violating gauge interactions, inducing at low energies a set of effective dimension six operators that conserve $B - L$. In the $SO(10)$ scenarios we consider here, such gauge bosons are integrated out at the unification scale, and therefore proton decay constrains n_U from below. The present experimental limit $\tau_p(p \rightarrow e^+ \pi^0) > 1.6 \times 10^{33}$ years [28] implies

$$\left(\frac{\alpha_U^{-1}}{45}\right) 10^{2(n_U - 15)} > 5.2, \tag{36}$$

which, for $\alpha_U^{-1} = 45$ yields $n_U > 15.4$. Taking the results

in Figs. 1 and 2 and Table III at face value the chains VIab, XIab, XIIab, Vb, and VIIb should be excluded from realistic considerations.

On the other hand, one must recall that once a specific model is scrutinized in detail there can be large threshold corrections in the matching [10–12], that can easily move the unification scale by a few orders of magnitude (in both directions). In particular, as a consequence of the spontaneous breaking of accidental would-be global symmetries of the scalar potential, pseudo-Goldstone modes (with masses further suppressed with respect to the expected threshold range) may appear in the scalar spectrum, leading to potentially large RGE effects [30]. Therefore, we shall follow a conservative approach in interpreting the limits on the intermediate scales coming from a simple threshold clustering. These limits, albeit useful for a preliminary survey, may not be sharply used to exclude marginal but otherwise well-motivated scenarios.

Below the scale of the $B-L$ breaking, processes that violate separately the baryon or the lepton numbers emerge. In particular, $\Delta B=2$ effective interactions give rise to the phenomenon of neutron oscillations (for a recent review see Ref. [31]). Present bounds on nuclear instability give $\tau_{\mathrm{Nucl}}>10^{32}$ years, which translates into a bound on the neutron oscillation time $\tau_{n-\bar{n}}>10^{8}$ sec. Analogous limits come from direct reactor oscillations experiments. This sets a lower bound on the scale of $\Delta B=2$ nonsupersymmetric (dimension nine) operators that varies from 10 to 300 TeV depending on model couplings. Thus, antineutron oscillations probe scales far below the unification scale. In a supersymmetric context the presence of $\Delta B=2$ dimension seven operators softens the dependence on the $B-L$ scale and for the present bounds the typical limit goes up to about 10^{7} GeV.

Far more reaching in scale sensitivity are the $\Delta L=2$ neutrino masses emerging from the seesaw mechanism. At the $B-L$ breaking scale the Δ_R^{126} (δ_R^{16}) scalars acquire $\Delta L=2$ ($\Delta L=1$) VEVs that give a Majorana mass to the right-handed neutrinos. Once the latter are integrated out, dimension five operators of the form $\bar{\nu}_L^c \nu_L H H^T$ generate light Majorana neutrino states in the low energy theory.

In the type-I seesaw, the neutrino mass matrix m_ν is proportional to $Y_N M_R^{-1} Y_N^T v^2$ where the largest entry in the Yukawa couplings is typically of the order of the top quark one and $M_R\sim M_1$. Given a neutrino mass above the limit obtained from atmospheric neutrino oscillations and below the eV, one infers a (loose) range $10^{12}\ \mathrm{GeV}<M_1<10^{14}\ \mathrm{GeV}$. It is interesting to note that the lower bound pairs with the cosmological limit on the D-parity breaking scale (see Sec. II).

In the scalar-triplet induced (type-II) seesaw the evidence of the neutrino mass entails a lower bound on the VEV of the heavy $SU(2)_L$ triplet in $\overline{126}_H$ (or in $\overline{16}_H\overline{16}_H$). This translates into an upper bound on the mass of the triplet that depends on the structure of the relevant Yukawa coupling. If both type-I as well as type-II contribute to the light neutrino mass, the lower bound on the M_1 scale may then be weakened by the interplay between the two contributions. Once again this can be quantitatively assessed only when the vacuum of the model is fully investigated.

Finally, it is worth noting that if the $B-L$ breakdown is driven by $\overline{126}_H$, the elementary triplets couple to the Majorana currents at the renormalizable level and m_ν is directly sensitive to the position of the $G1\to SM$ threshold M_1. On the other hand, the n_1 dependence of m_ν is loosened in the b-type of chains due to the nonrenormalizable nature of the relevant effective operator $16_F 16_F \overline{16}_H \overline{16}_H/\Lambda$, where the effective scale $\Lambda>M_U$ accounts for an extra suppression.

With these considerations at hand, the constraints from proton decay and the seesaw neutrino scale favor the chains II, III, and VII, which all share $2_L 2_R 4_C P$ in the first $SO(10)$ breaking stage [5]. On the other hand, our results rescue from oblivion other potentially interesting scenarios that, as we shall expand upon shortly, are worth in-depth consideration. In all cases, the bounds on the $B-L$ scale enforced by the seesaw neutrino mass excludes the possibility of observable $U(1)_R$ gauge bosons.

C. The ϕ^{126} Higgs multiplets

As mentioned in Sec. II A, in order to ensure a rich enough Yukawa sector in realistic models there may be the need to keep more than one $SU(2)_L$ Higgs doublet at intermediate scales, albeit at the price of an extra fine-tuning. A typical example is the case of a relatively low Pati-Salam breaking scale where one needs at least a pair of $SU(2)_L\otimes SU(2)_R$ bidoublets with different $SU(4)_C$ quantum numbers to transfer the information about the PS breakdown into the matter sector. Such additional Higgs multiplets are those labeled by ϕ^{126} in Table II.

Table IV shows the effects of including ϕ^{126} at the $SU(4)_C$ stages of the relevant breaking chains. The two-loop results at the extreme values of the intermediate scales, with and without the ϕ^{126} multiplet, are compared. In the latter case the complete functional dependence among the scales is given in Fig. 1. Degenerate patterns with only one effective intermediate stage are easily cross-checked among the different chains in Table IV.

In most of the cases, the numerical results do not exhibit a sizeable dependence on the additional $(2,2,15)_{\overline{126}}$ (or $(2,+\frac{1}{2},15)_{\overline{126}}$) scalar multiplets. The reason can be read off Table X in Appendix A and it rests on an accidental approximate coincidence of the ϕ^{126} contributions to the $SU(4)_C$ and $SU(2)_{L,R}$ one-loop beta coefficients (the same argument applies to the $2_L 1_R 4_C$ case).

Considering, for instance, the $2_L 2_R 4_C$ stage, one obtains $\Delta a_4=\frac{1}{3}\times 4\times T_2(15)=\frac{16}{3}$, and $\Delta a_2=\frac{1}{3}\times 30\times T_2(2)=5$, that only slightly affects the value of α_U (when the PS scale is low enough), but has generally a negligible effect on the intermediate scales.

TABLE IV. Impact of the additional multiplet ϕ^{126} (second line of each chain) on those chains that contain the gauge groups $2_L 2_R 4_C$ or $2_L 1_R 4_C$ as intermediate stages, and whose breaking to the SM is obtained via a $\overline{126}_H$ representation. The values of n_2, n_U, and α_U^{-1} are showed for the minimum and maximum values allowed for n_1 by the two-loop analysis. Generally the effects on the intermediate scales are below the percent level, with the exception of chains Ia and Va that are most sensitive to variations of the β functions.

Chain	n_1	n_2	n_U	α_U^{-1}
Ia	[9.50, 10.0]	[16.2, 10.0]	[16.2, 17.0]	[45.5, 46.4]
	[8.00, 9.50]	[10.4, 16.2]	[18.0, 16.2]	[30.6, 45.5]
IIa	[10.5, 13.7]	[15.4, 13.7]	[15.4, 15.1]	[43.7, 40.8]
	[10.5, 13.7]	[15.4, 13.7]	[15.4, 15.1]	[43.7, 37.6]
IIIa	[9.50, 13.7]	[16.2, 13.7]	[16.2, 15.1]	[45.5, 40.8]
	[9.50, 13.7]	[16.2, 13.7]	[16.2, 15.1]	[45.5, 37.6]
Va	[11.0, 11.4]	[11.0, 14.4]	[15.9, 14.4]	[45.4, 44.1]
	[10.1, 11.2]	[10.1, 14.5]	[16.5, 14.5]	[32.5, 40.8]
VIa	[11.4, 13.7]	[14.4, 13.7]	[14.4, 14.9]	[44.1, 41.0]
	[11.2, 13.7]	[14.5, 13.7]	[14.5, 14.9]	[40.8, 38.1]
VIIa	[11.3, 13.7]	[15.9, 13.7]	[15.9, 14.9]	[45.4, 41.1]
	[10.5, 13.7]	[16.5, 13.7]	[16.5, 15.0]	[33.3, 38.1]
XIa	[3.00, 13.7]	[13.7, 13.7]	[14.8, 14.8]	[38.7, 38.7]
	[3.00, 13.7]	[13.7, 13.7]	[14.8, 14.8]	[36.0, 36.0]
XIIa	[3.00, 10.8]	[10.8, 10.8]	[14.6, 14.6]	[44.1, 44.1]
	[3.00, 10.5]	[10.5, 10.5]	[14.7, 14.7]	[39.8, 39.8]

An exception to this argument is observed in chains Ia and Va that, due to their $n_{2,U}(n_1)$ slopes, are most sensitive to variations of the β coefficients. In particular, the inclusion of ϕ^{126} in the Ia chain flips at two loops the slopes of n_2 and n_U so that the limit $n_2 = n_U$ (i.e. no $G2$ stage) is obtained for the maximal value of n_1 (while the same happens for the minimum n_1 if there is no ϕ^{126}).

Figure 3 shows three template cases where the ϕ^{126} effects are visible. The highly unstable chain Ia shows, as noticed earlier, the largest effects. In chain Va the effects of ϕ^{126} are moderate. Chain VII is the only "stable" chain that exhibits visible effects on the intermediate scales. This is due to the presence of two full-fledged PS stages.

D. Yukawa terms

The effects of the Yukawa couplings can be at leading order approximated by constant negative shifts of the one-loop a_i coefficients $a_i \to a_i' = a_i + \Delta a_i$ with

$$\Delta a_i = -\frac{1}{(4\pi)^2} y_{ik} \,\mathrm{Tr}\, Y_k Y_k^\dagger. \tag{37}$$

The impact of Δa_i on the position of the unification scale and the value of the unified coupling can be simply estimated by considering the running induced by the Yukawa couplings from a scale t up to the unification point ($t = 0$). The one-loop result for the change of the intersection of the curves corresponding to $\alpha_i^{-1}(t)$ and $\alpha_j^{-1}(t)$ reads (at the leading order in Δa_i):

$$\Delta t_U = 2\pi \frac{\Delta a_i - \Delta a_j}{(a_i - a_j)^2} [\alpha_j^{-1}(t) - \alpha_i^{-1}(t)] + \ldots \tag{38}$$

and

$$\Delta \alpha_U^{-1} = \frac{1}{2}\left[\frac{\Delta a_i + \Delta a_j}{a_i - a_j} - \frac{(a_i + a_j)(\Delta a_i - \Delta a_j)}{(a_i - a_j)^2}\right] \times [\alpha_j^{-1}(t) - \alpha_i^{-1}(t)] + \ldots \tag{39}$$

for any $i \neq j$. For simplicity we have neglected the changes in the a_i coefficients due to crossing intermediate thresholds. It is clear that for a common change $\Delta a_i = \Delta a_j$ the unification scale is not affected, while a net effect remains on α_U^{-1}. In all cases, the leading contribution is always proportional to $\alpha_j^{-1}(t) - \alpha_i^{-1}(t)$ (this holds exactly for Δt_U).

In order to assess quantitatively such effects we shall consider first the SM stage that accounts for a large part of the running in all realistic chains. The case of a low n_1 scale leads, as we explain in the following, to comparably smaller effects. The impact of the Yukawa interactions on the gauge RGEs is readily estimated assuming only the up-type Yukawa contribution to be sizeable and constant, namely $\mathrm{Tr} Y_U Y_U^\dagger \sim 1$. This yields $\Delta a_i \sim -6 \times 10^{-3} y_{iU}$, where the values of the y_{iU} coefficients are given in Table XI. For $i = 1$ and $j = 2$ one obtains $\Delta a_1 \sim -1.1 \times 10^{-2}$ and

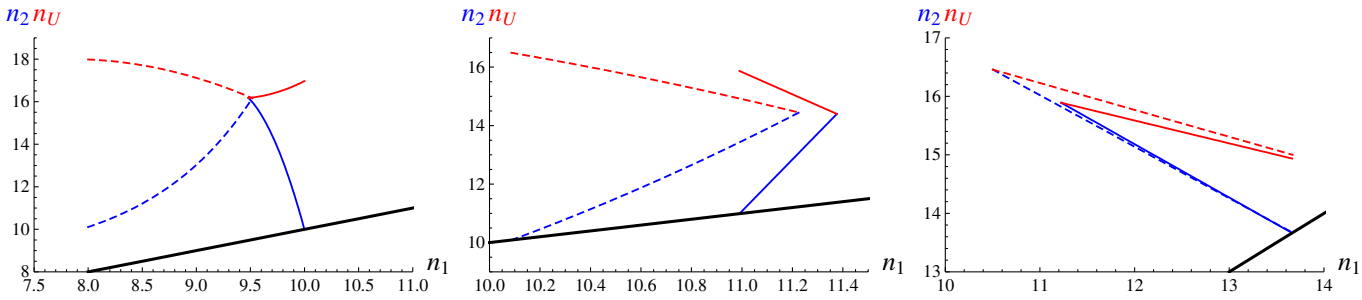

(a) Chain Ia (b) Chain Va (c) Chain VIIa

FIG. 3 (color online). Example of chains with sizeable ϕ^{126} effects (long-dashed curves) on the position of the intermediate scales. The solid curves represent the two-loop results in Fig. 1. The most dramatic effects appear in the chain Ia, while moderate scale shifts affect chain Va (both unstable under small variations of the β functions). Chain VIIa, due to the presence of two PS stages, is the only stable chain with visible ϕ^{126} effects.

$\Delta a_2 \sim -0.9 \times 10^{-2}$, respectively. Since $a_1^{\rm SM} = \frac{41}{10}$ and $a_2^{\rm SM} = -\frac{19}{6}$, the first term in (39) dominates and one finds $\Delta\alpha_U^{-1} \sim 0.04$. For a typical value of $\alpha_U^{-1} \sim 40$ this translates into $\Delta\alpha_U^{-1}/\alpha_U^{-1} \sim 0.1\%$. The impact on t_U is indeed tiny, namely $\Delta n_U \sim -1 \times 10^{-2}$. In both cases the estimated effect agrees to high accuracy with the actual numerical behavior we observe.

The effects of the Yukawa interactions emerging at intermediate scales (or of a non-negligible $\mathrm{Tr}\, Y_D Y_D^\dagger$ in a two Higgs doublet setting with large $\tan\beta$) can be analogously accounted for. As a matter of fact, in the $SO(10)$ type of models $\mathrm{Tr}\, Y_N Y_N^\dagger \sim \mathrm{Tr}\, Y_U Y_U^\dagger$ due to the common origin of Y_U and Y_N. The unified structure of the Yukawa sector yields therefore homogeneous Δa_i factors (see the equality of $\sum_k y_{ik}$ in Table XI). This provides the observed large suppression of the Yukawa effects on threshold scales and unification compared to typical two-loop gauge contributions.

In summary, the two-loop RGE effects due to Yukawa couplings on the magnitude of the unification scale (and intermediate thresholds) and the value of the GUT gauge coupling turn out to be very small. Typically we observe negative shifts at the per-mil level in both n_U and α_U, with no relevant impact on the gauge-mediated proton decay rate.

E. The privilege of being minimal

With all the information at hand we can finally approach an assessment of the viability of the various scenarios. As we have argued at length, we cannot discard a marginal unification setup without detailed information on the fine threshold structure.

Obtaining this piece of information involves the study of the vacuum of the model, and for $SO(10)$ GUTs this is in general a most challenging task. In this respect supersymmetry helps: the superpotential is holomorphic and the couplings in the renormalizable case are limited to at most cubic terms; the physical vacuum is constrained by GUT-scale F and D flatness and supersymmetry may be exploited to studying the fermionic rather than the scalar spectra.

It is not surprising that for nonsupersymmetric $SO(10)$, only a few detailed studies of the Higgs potential and the related threshold effects (see for instance Refs. [32–36]) are available. In view of all this and of the intrinsic predictivity related to minimality, the relevance of carefully scrutinizing the simplest scenarios is hardly overstressed.

The most economical $SO(10)$ Higgs sector includes the adjoint 45_H, that provides the breaking of the GUT symmetry, either $\overline{16}_H$ or $\overline{126}_H$, responsible for the subsequent $B-L$ breaking, and 10_H, participating to the electroweak symmetry breaking. The latter is needed together with $\overline{16}_H$ or $\overline{126}_H$ in order to obtain realistic patterns for the fermionic masses and mixing. Because of the properties of the adjoint representation this scenario exhibits a minimal number of parameters in the Higgs potential. In the current notation such a *minimal nonsupersymmetric* $SO(10)$ (MSO10) GUT corresponds to the chains VIII and XII.

From this point of view, it is quite intriguing that our analysis of the gauge unification constraints improves the standing of these chains (for XIIa dramatically) with respect to existing studies. In particular, considering the renormalizable setups ($\overline{126}_H$), we find for chain VIIIa, $n_1 \leq 9.1$, $n_U = 16.2$, and $\alpha_U^{-1} = 45.4$ (to be compared to $n_1 \leq 7.7$ given in Ref. [9]). This is due to the combination of the updated weak scale data and two-loop running effects. For chain XIIa we find $n_1 \leq 10.8$, $n_U = 14.6$, and $\alpha_U^{-1} = 44.1$, showing a dramatic (and pathological) change from $n_1 \leq 5.3$ obtained in [9]. Our result sets the $B-L$ scale nearby the needed scale for realistic light neutrino masses.

We observe non-negligible two-loop effects for the chains VIIIb and XIIb ($\overline{16}_H$) as well. For chain VIIIb we obtain $n_1 \leq 10.5$, $n_U = 16.2$, and $\alpha_U^{-1} = 45.6$ (that lifts the $B-L$ scale while preserving n_U well above the proton decay bound Eq. (36)). A similar shift in n_1 is observed in chain XIIb where we find $n_1 \leq 12.5$, $n_U = 14.8$, and $\alpha_U^{-1} = 44.3$. As we have already stressed one should not too readily discard $n_U = 14.8$ as being incompatible with the proton decay bound. We have verified that reasonable GUT threshold patterns exist that easily lift n_U above the experimental bound. For all these chains D parity is broken at the GUT scale thus avoiding any cosmological issues (see the discussion in Sec. II).

As remarked in Sec. IV B, the limit $n_1 = n_2$ leads to an effective two-step $SO(10) \to G2 \to \mathrm{SM}$ scenario with a *nonminimal* set of surviving scalars at the $G2$ stage. As a consequence, the unification setup for the MSO10 can be recovered (with the needed minimal fine-tuning) by considering the limit $n_2 = n_U$ in those chains among I to VII where $G1$ is either $2_L 2_R 1_X 3_c$ or $2_L 1_R 4_C$ (see Table I). From the inspection of Figs. 1 and 2 and of Table III, one reads the following results: for $SO(10) \to {}_{45}2_L 2_R 1_X 3_c \to \mathrm{SM}$ we find

$$n_1 = 9.5, \quad n_U = 16.2, \quad \text{and} \quad \alpha_U^{-1} = 45.5, \quad \text{in case } a$$

and

$$n_1 = 10.8, \quad n_U = 16.2, \quad \text{and} \quad \alpha_U^{-1} = 45.7, \quad \text{in case } b,$$

while for $SO(10) \to {}_{45}2_L 1_R 4_C \to \mathrm{SM}$

$$n_1 = 11.4, \quad n_U = 14.4, \quad \text{and} \quad \alpha_U^{-1} = 44.1, \quad \text{in case } a$$

and

$$n_1 = 12.6, \quad n_U = 14.6, \quad \text{and} \quad \alpha_U^{-1} = 44.3, \quad \text{in case } b.$$

We observe that the patterns are quite similar to those of the nonminimal setups obtained from chains VIII and XII in the $n_1 = n_2$ limit. Adding the ϕ^{126} multiplet, as required by a realistic matter spectrum in case a, does not modify the scalar content in the $2_L 2_R 1_X 3_c$ case: only one linear combination of the 10_H and $\overline{126}_H$ bidoublets (see Table II)

is allowed by minimal fine-tuning. On the other hand, in the $2_L 1_R 4_C$ case, the only sizeable effect is a shift on the unified coupling constant, namely $\alpha_U^{-1} = 40.7$ (see the discussion in Sec. IV C).

In summary, in view of realistic thresholds effects at the GUT (and $B - L$) scale and of a modest fine-tuning in the seesaw neutrino mass, we consider both scenarios worth a detailed investigation.

V. OUTLOOK

We presented an updated and systematic two-loop discussion of nonsupersymmetric $SO(10)$ gauge unification with two (and one) intermediate scales. We completed and corrected existing analyses by including a thorough discussion of $U(1)$ mixing, which affects the gauge running already at the one-loop level in a number of interesting $SO(10)$ breaking chains. We assessed the relevance of additional Higgs multiplets, needed at some of the intermediate stages in order to reproduce a realistic fermionic mass spectrum. Finally, we found and fixed several discrepancies in the two-loop β coefficients.

The updated results have a non-negligible impact on the values of the unification and $B - L$ scales (as well as on the value of the unified gauge coupling). This is due to the combined effects of the one-loop dynamics corresponding to the $U(1)$ gauge mixing and of the two-loop RGE contributions.

We discussed the viability of the different $SO(10)$ scenarios on the basis of proton decay and the seesaw induced neutrino mass. We were lead to focus our attention on the minimal $SO(10)$ setup, emerging from a balance of minimal dimensionality Higgs representations and a minimal number of parameters in the scalar potential. Such a scenario invokes, in addition to a complex 10_H, one adjoint 45_H together with one $\overline{126}_H$ or $\overline{16}_H$ at the effective level.

Although the updated values of the unification or $B - L$ scales are in some of the setups still conflicting with the experimental requirements, they are close enough that reasonable spreads in the GUT thresholds (or a moderate fine-tuning in the neutrino mass matrix) can easily restore the agreement. This may entail the detailed study of the scalar potential of the model beyond the tree approximation, that is a rather nontrivial task. Nevertheless, the appeal of minimality (with supersymmetry confined to the Planck scale) motivates us to pursue this study.

ACKNOWLEDGMENTS

S. B. acknowledges support by MIUR and by the RTN European Program MRTN-CT-2004-503369. The work of M. M. is supported by the Royal Institute of Technology (KTH), Contract No. SII-56510. M. M. is grateful to SISSA for the hospitality during the preparation of part of the manuscript.

APPENDIX A: ONE- AND TWO-LOOP BETA COEFFICIENTS

In Tables V, VI, VII, VIII, IX, X, and XI we report the one- and two-loop β coefficients used in the numerical

TABLE V. The a_i and b_{ij} coefficients due to pure gauge interactions are reported for the $G2$ chains with $\overline{126}_H$ (left) and 16_H (right), respectively. The two-loop contributions induced by Yukawa couplings are discussed in Appendix A 2.

$G2$ ($M_U \to M_2$)

Chain	a_j	b_{ij}	Chain	a_j	b_{ij}
Ia	$(-3, \frac{11}{3}, -7)$	$\begin{pmatrix} 8 & 3 & \frac{45}{2} \\ 3 & \frac{584}{3} & \frac{765}{2} \\ \frac{9}{2} & \frac{153}{2} & \frac{289}{2} \end{pmatrix}$	Ib	$(-3, -\frac{7}{3}, -\frac{29}{3})$	$\begin{pmatrix} 8 & 3 & \frac{45}{2} \\ 3 & \frac{50}{3} & \frac{75}{2} \\ \frac{9}{2} & \frac{15}{2} & -\frac{94}{3} \end{pmatrix}$
IIa	$(\frac{11}{3}, \frac{11}{3}, -4)$	$\begin{pmatrix} \frac{584}{3} & 3 & \frac{765}{2} \\ 3 & \frac{584}{3} & \frac{765}{2} \\ \frac{153}{2} & \frac{153}{2} & \frac{661}{2} \end{pmatrix}$	IIb	$(-\frac{7}{3}, -\frac{7}{3}, -\frac{28}{3})$	$\begin{pmatrix} \frac{50}{3} & 3 & \frac{75}{2} \\ 3 & \frac{50}{3} & \frac{75}{2} \\ \frac{15}{2} & \frac{15}{2} & -\frac{127}{6} \end{pmatrix}$
IIIa	$(\frac{11}{3}, \frac{11}{3}, -4)$	$\begin{pmatrix} \frac{584}{3} & 3 & \frac{765}{2} \\ 3 & \frac{584}{3} & \frac{765}{2} \\ \frac{153}{2} & \frac{153}{2} & \frac{661}{2} \end{pmatrix}$	IIIb	$(-\frac{7}{3}, -\frac{7}{3}, -\frac{28}{3})$	$\begin{pmatrix} \frac{50}{3} & 3 & \frac{75}{2} \\ 3 & \frac{50}{3} & \frac{75}{2} \\ \frac{15}{2} & \frac{15}{2} & -\frac{127}{6} \end{pmatrix}$
IVa	$(-\frac{7}{3}, -\frac{7}{3}, 7, -7)$	$\begin{pmatrix} \frac{80}{3} & 3 & \frac{27}{2} & 12 \\ 3 & \frac{80}{3} & \frac{27}{2} & 12 \\ \frac{81}{2} & \frac{81}{2} & \frac{115}{2} & 4 \\ \frac{9}{2} & \frac{9}{2} & \frac{1}{2} & -26 \end{pmatrix}$	IVb	$(-\frac{17}{6}, -\frac{17}{6}, \frac{9}{2}, -7)$	$\begin{pmatrix} \frac{61}{6} & 3 & \frac{9}{4} & 12 \\ 3 & \frac{61}{6} & \frac{9}{4} & 12 \\ \frac{27}{4} & \frac{27}{4} & \frac{23}{4} & 4 \\ \frac{9}{2} & \frac{9}{2} & \frac{1}{2} & -26 \end{pmatrix}$
Va	$(-3, 4, -\frac{23}{3})$	$\begin{pmatrix} 8 & 3 & \frac{45}{2} \\ 3 & 204 & \frac{765}{2} \\ \frac{9}{2} & \frac{153}{2} & \frac{643}{6} \end{pmatrix}$	Vb	$(-3, -2, -\frac{31}{3})$	$\begin{pmatrix} 8 & 3 & \frac{45}{2} \\ 3 & 26 & \frac{75}{2} \\ \frac{9}{2} & \frac{15}{2} & -\frac{206}{3} \end{pmatrix}$
VIa	$(4, 4, -\frac{14}{3})$	$\begin{pmatrix} 204 & 3 & \frac{765}{2} \\ 3 & 204 & \frac{765}{2} \\ \frac{153}{2} & \frac{153}{2} & \frac{1759}{6} \end{pmatrix}$	VIb	$(-2, -2, -10)$	$\begin{pmatrix} 26 & 3 & \frac{75}{2} \\ 3 & 26 & \frac{75}{2} \\ \frac{15}{2} & \frac{15}{2} & -\frac{117}{2} \end{pmatrix}$

TABLE V. (*Continued*)

$G2$ ($M_U \to M_2$)

Chain	a_j	b_{ij}	Chain	a_j	b_{ij}
VIIa	$(\frac{11}{3}, \frac{11}{3}, -\frac{14}{3})$	$\begin{pmatrix} \frac{584}{3} & 3 & \frac{765}{2} \\ 3 & \frac{584}{3} & \frac{765}{2} \\ \frac{153}{2} & \frac{153}{2} & \frac{1759}{6} \end{pmatrix}$	VIIb	$(-\frac{7}{3}, -\frac{7}{3}, -10)$	$\begin{pmatrix} \frac{50}{3} & 3 & \frac{75}{2} \\ 3 & \frac{50}{3} & \frac{75}{2} \\ \frac{15}{2} & \frac{15}{2} & -\frac{117}{2} \end{pmatrix}$
VIIIa	$(-3, -2, \frac{11}{2}, -7)$	$\begin{pmatrix} 8 & 3 & \frac{3}{2} & 12 \\ 3 & 36 & \frac{27}{2} & 12 \\ \frac{9}{2} & \frac{81}{2} & \frac{61}{2} & 4 \\ \frac{9}{2} & \frac{9}{2} & \frac{1}{2} & -26 \end{pmatrix}$	VIIIb	$(-3, -\frac{5}{2}, \frac{17}{4}, -7)$	$\begin{pmatrix} 8 & 3 & \frac{3}{2} & 12 \\ 3 & \frac{39}{2} & \frac{9}{4} & 12 \\ \frac{9}{2} & \frac{27}{2} & \frac{37}{8} & 4 \\ \frac{9}{2} & \frac{9}{2} & \frac{1}{2} & -26 \end{pmatrix}$
IXa	$(-2, -2, 7, -7)$	$\begin{pmatrix} 36 & 3 & \frac{27}{2} & 12 \\ 3 & 36 & \frac{27}{2} & 12 \\ \frac{81}{2} & \frac{81}{2} & \frac{115}{2} & 4 \\ \frac{9}{2} & \frac{9}{2} & \frac{1}{2} & -26 \end{pmatrix}$	IXb	$(-\frac{5}{2}, -\frac{5}{2}, \frac{9}{2}, -7)$	$\begin{pmatrix} \frac{39}{2} & 3 & \frac{9}{4} & 12 \\ 3 & \frac{39}{2} & \frac{9}{4} & 12 \\ \frac{27}{4} & \frac{27}{4} & \frac{23}{4} & 4 \\ \frac{9}{2} & \frac{9}{2} & \frac{1}{2} & -26 \end{pmatrix}$
Xa	$(-3, \frac{26}{3}, -\frac{17}{3})$	$\begin{pmatrix} 8 & 3 & \frac{45}{2} \\ 3 & \frac{1004}{3} & \frac{1245}{2} \\ \frac{9}{2} & \frac{249}{2} & \frac{1315}{6} \end{pmatrix}$	Xb	$(-3, \frac{8}{3}, -\frac{25}{3})$	$\begin{pmatrix} 8 & 3 & \frac{45}{2} \\ 3 & \frac{470}{3} & \frac{555}{2} \\ \frac{9}{2} & \frac{111}{2} & \frac{130}{3} \end{pmatrix}$
XIa	$(\frac{26}{3}, \frac{26}{3}, -\frac{2}{3})$	$\begin{pmatrix} \frac{1004}{3} & 3 & \frac{1245}{2} \\ 3 & \frac{1004}{3} & \frac{1245}{2} \\ \frac{249}{2} & \frac{249}{2} & \frac{3103}{6} \end{pmatrix}$	XIb	$(\frac{8}{3}, \frac{8}{3}, -6)$	$\begin{pmatrix} \frac{470}{3} & 3 & \frac{555}{2} \\ 3 & \frac{470}{3} & \frac{555}{2} \\ \frac{111}{2} & \frac{111}{2} & \frac{331}{2} \end{pmatrix}$
XIIa	$(-\frac{19}{6}, \frac{15}{2}, -9)$	$\begin{pmatrix} \frac{35}{6} & \frac{1}{2} & \frac{45}{2} \\ \frac{3}{2} & \frac{87}{2} & \frac{405}{2} \\ \frac{9}{2} & \frac{27}{2} & \frac{41}{2} \end{pmatrix}$	XIIb	$(-\frac{19}{6}, \frac{9}{2}, -\frac{59}{6})$	$\begin{pmatrix} \frac{35}{6} & \frac{1}{2} & \frac{45}{2} \\ \frac{3}{2} & \frac{9}{2} & 30 \\ \frac{9}{2} & 2 & -\frac{437}{12} \end{pmatrix}$

TABLE VI. The a_i and b_{ij} coefficients due to gauge interactions are reported for the $G1$ chains I to VII with $\overline{126}_H$ (left) and $\overline{16}_H$ (right), respectively. The two-loop contributions induced by Yukawa couplings are discussed in Appendix A 2.

$G1$ ($M_2 \to M_1$)

Chain	a_i	b_{ij}	Chain	a_i	b_{ij}
Ia	$(-3, -\frac{7}{3}, \frac{11}{2}, -7)$	$\begin{pmatrix} 8 & 3 & \frac{3}{2} & 12 \\ 3 & \frac{80}{3} & \frac{27}{2} & 12 \\ \frac{9}{2} & \frac{81}{2} & \frac{61}{2} & 4 \\ \frac{9}{2} & \frac{9}{2} & \frac{1}{2} & -26 \end{pmatrix}$	Ib	$(-3, -\frac{17}{6}, \frac{17}{4}, -7)$	$\begin{pmatrix} 8 & 3 & \frac{3}{2} & 12 \\ 3 & \frac{61}{6} & \frac{9}{4} & 12 \\ \frac{9}{2} & \frac{27}{2} & \frac{37}{8} & 4 \\ \frac{9}{2} & \frac{9}{2} & \frac{1}{2} & -26 \end{pmatrix}$
IIa	$(-\frac{7}{3}, -\frac{7}{3}, 7, -7)$	$\begin{pmatrix} \frac{80}{3} & 3 & \frac{27}{2} & 12 \\ 3 & \frac{80}{3} & \frac{27}{2} & 12 \\ \frac{81}{2} & \frac{81}{2} & \frac{115}{2} & 4 \\ \frac{9}{2} & \frac{9}{2} & \frac{1}{2} & -26 \end{pmatrix}$	IIb	$(-\frac{17}{6}, -\frac{17}{6}, \frac{9}{2}, -7)$	$\begin{pmatrix} \frac{61}{6} & 3 & \frac{9}{4} & 12 \\ 3 & \frac{61}{6} & \frac{9}{4} & 12 \\ \frac{27}{4} & \frac{27}{4} & \frac{23}{4} & 4 \\ \frac{9}{2} & \frac{9}{2} & \frac{1}{2} & -26 \end{pmatrix}$
IIIa	$(-3, -\frac{7}{3}, \frac{11}{2}, -7)$	$\begin{pmatrix} 8 & 3 & \frac{3}{2} & 12 \\ 3 & \frac{80}{3} & \frac{27}{2} & 12 \\ \frac{9}{2} & \frac{81}{2} & \frac{61}{2} & 4 \\ \frac{9}{2} & \frac{9}{2} & \frac{1}{2} & -26 \end{pmatrix}$	IIIb	$(-3, -\frac{17}{6}, \frac{17}{4}, -7)$	$\begin{pmatrix} 8 & 3 & \frac{3}{2} & 12 \\ 3 & \frac{61}{6} & \frac{9}{4} & 12 \\ \frac{9}{2} & \frac{27}{4} & \frac{37}{8} & 4 \\ \frac{9}{2} & \frac{9}{2} & \frac{1}{2} & -26 \end{pmatrix}$
IVa	$(-3, -\frac{7}{3}, \frac{11}{2}, -7)$	$\begin{pmatrix} 8 & 3 & \frac{3}{2} & 12 \\ 3 & \frac{80}{3} & \frac{27}{2} & 12 \\ \frac{9}{2} & \frac{81}{2} & \frac{61}{2} & 4 \\ \frac{9}{2} & \frac{9}{2} & \frac{1}{2} & -26 \end{pmatrix}$	IVb	$(-3, -\frac{17}{6}, \frac{17}{4}, -7)$	$\begin{pmatrix} 8 & 3 & \frac{3}{2} & 12 \\ 3 & \frac{61}{6} & \frac{9}{4} & 12 \\ \frac{9}{2} & \frac{27}{4} & \frac{37}{8} & 4 \\ \frac{9}{2} & \frac{9}{2} & \frac{1}{2} & -26 \end{pmatrix}$
Va	$(-\frac{19}{6}, \frac{15}{2}, -\frac{29}{3})$	$\begin{pmatrix} \frac{35}{6} & \frac{1}{2} & \frac{45}{2} \\ \frac{3}{2} & \frac{87}{2} & \frac{405}{2} \\ \frac{9}{2} & \frac{27}{2} & -\frac{101}{6} \end{pmatrix}$	Vb	$(-\frac{19}{6}, \frac{9}{2}, -\frac{21}{2})$	$\begin{pmatrix} \frac{35}{6} & \frac{1}{2} & \frac{45}{2} \\ \frac{3}{2} & \frac{9}{2} & 30 \\ \frac{9}{2} & 2 & -\frac{295}{4} \end{pmatrix}$
VIa	$(-\frac{19}{6}, \frac{15}{2}, -\frac{29}{3})$	$\begin{pmatrix} \frac{35}{6} & \frac{1}{2} & \frac{45}{2} \\ \frac{3}{2} & \frac{87}{2} & \frac{405}{2} \\ \frac{9}{2} & \frac{27}{2} & -\frac{101}{6} \end{pmatrix}$	VIb	$(-\frac{19}{6}, \frac{9}{2}, -\frac{21}{2})$	$\begin{pmatrix} \frac{35}{6} & \frac{1}{2} & \frac{45}{2} \\ \frac{3}{2} & \frac{9}{2} & 30 \\ \frac{9}{2} & 2 & -\frac{295}{4} \end{pmatrix}$
VIIa	$(-3, \frac{11}{3}, -\frac{23}{3})$	$\begin{pmatrix} 8 & 3 & \frac{45}{2} \\ 3 & \frac{584}{3} & \frac{765}{2} \\ \frac{9}{2} & \frac{153}{2} & \frac{643}{6} \end{pmatrix}$	VIIb	$(-3, -\frac{7}{3}, -\frac{31}{3})$	$\begin{pmatrix} 8 & 3 & \frac{45}{2} \\ 3 & \frac{50}{3} & \frac{75}{2} \\ \frac{9}{2} & \frac{15}{2} & -\frac{206}{3} \end{pmatrix}$

TABLE VII. The a_i and b_{ij} coefficients due to purely gauge interactions for the $G1$ chains VIII to XII are reported. For comparison with previous studies the β coefficients are given neglecting systematically one- and two-loops $U(1)$ mixing effects (while all diagonal $U(1)$ contributions to Abelian and non-Abelian gauge coupling renormalization are included). The complete (and correct) treatment of $U(1)$ mixing is detailed in Appendix A 1.

$G1$ $(M_2 \to M_1)$

Chain	a_i	b_{ij}	Chain	a_i	b_{ij}
VIIIa ⋮ XIIa	$(-\frac{19}{6}, \frac{9}{2}, \frac{9}{2}, -7)$	$\begin{pmatrix} \frac{35}{6} & \frac{1}{2} & \frac{3}{2} & 12 \\ \frac{3}{2} & \frac{15}{2} & \frac{15}{2} & 12 \\ \frac{9}{2} & \frac{15}{2} & \frac{25}{2} & 4 \\ \frac{9}{2} & \frac{3}{2} & \frac{1}{2} & -26 \end{pmatrix}$	VIIIb ⋮ XIIb	$(-\frac{19}{6}, \frac{17}{4}, \frac{33}{8}, -7)$	$\begin{pmatrix} \frac{35}{6} & \frac{1}{2} & \frac{3}{2} & 12 \\ \frac{3}{2} & \frac{15}{4} & \frac{15}{8} & 12 \\ \frac{9}{2} & \frac{15}{8} & \frac{65}{16} & 4 \\ \frac{9}{2} & \frac{3}{2} & \frac{1}{2} & -26 \end{pmatrix}$

TABLE VIII. The a_i and b_{ij} coefficients are given for the $1_Y 2_L 3_c$ (SM) gauge running. The scalar sector includes one Higgs doublet.

SM $(M_1 \to M_Z)$

Chain	a_i	b_{ij}
All	$(\frac{41}{10}, -\frac{19}{6}, -7)$	$\begin{pmatrix} \frac{199}{50} & \frac{27}{10} & \frac{44}{5} \\ \frac{9}{10} & \frac{35}{6} & 12 \\ \frac{11}{10} & \frac{9}{2} & -26 \end{pmatrix}$

TABLE X. One- and two-loop additional contributions to the β coefficients related to the presence of the ϕ^{126} scalar multiplets in the $2_L 2_R 4$ (top) and $2_L 1_R 4$ (bottom) stages.

ϕ^{126}	a_i	b_{ij}
(2, 2, 15)	$(5, 5, \frac{16}{3})$	$\begin{pmatrix} 65 & 45 & 240 \\ 45 & 65 & 240 \\ 48 & 48 & \frac{896}{3} \end{pmatrix}$
$(2, +\frac{1}{2}, 15)$	$(\frac{5}{2}, \frac{5}{2}, \frac{8}{3})$	$\begin{pmatrix} \frac{65}{2} & \frac{15}{2} & 120 \\ \frac{45}{2} & \frac{15}{2} & 120 \\ 24 & 8 & \frac{448}{3} \end{pmatrix}$

TABLE IX. The rescaled two-loop β coefficients $\tilde{b}_{ij}$ computed in this paper are shown together with the corresponding equations in Ref. [7]. For the purpose of comparison Yukawa contributions are neglected and no $U(1)$ mixing is included in chain VIIIa/$G1$. Care must be taken of the different ordering between Abelian and non-Abelian gauge group factors in Ref. [7]. We report those cases where disagreement is found in some of the entries, while we fully agree with the Eqs. A9, A11, and A16.

Chain	$\tilde{b}_{ij}$	Eq. in Ref. [7]
All/SM	$\begin{pmatrix} \frac{199}{205} & -\frac{81}{95} & -\frac{44}{35} \\ \frac{9}{41} & -\frac{35}{19} & -\frac{12}{7} \\ \frac{11}{41} & -\frac{27}{19} & \frac{26}{7} \end{pmatrix}$	A7
VIIIa/$G1$	$\begin{pmatrix} \frac{25}{9} & \frac{5}{3} & -\frac{27}{19} & -\frac{4}{7} \\ \frac{5}{3} & \frac{5}{3} & -\frac{9}{19} & -\frac{12}{7} \\ \frac{1}{3} & \frac{1}{3} & -\frac{35}{19} & -\frac{12}{7} \\ \frac{1}{9} & \frac{1}{3} & -\frac{27}{19} & \frac{26}{7} \end{pmatrix}$	A10
VIIIa/$G2$	$\begin{pmatrix} \frac{61}{11} & -\frac{3}{2} & -\frac{81}{4} & -\frac{4}{7} \\ \frac{3}{11} & -\frac{8}{3} & -\frac{3}{2} & -\frac{12}{7} \\ \frac{27}{11} & -1 & -18 & -\frac{12}{7} \\ \frac{1}{11} & -\frac{3}{2} & -\frac{9}{4} & \frac{26}{7} \end{pmatrix}$	A13
Ia/$G2$	$\begin{pmatrix} -\frac{8}{3} & \frac{9}{11} & -\frac{45}{14} \\ -1 & \frac{584}{11} & -\frac{765}{14} \\ -\frac{3}{2} & \frac{459}{22} & -\frac{289}{14} \end{pmatrix}$	A14
Va/$G1$	$\begin{pmatrix} -\frac{35}{19} & \frac{1}{15} & -\frac{135}{58} \\ -\frac{9}{19} & \frac{29}{5} & -\frac{1215}{58} \\ -\frac{27}{19} & \frac{9}{5} & \frac{101}{58} \end{pmatrix}$	A15
XIIa/$G2$	$\begin{pmatrix} -\frac{35}{19} & \frac{1}{15} & -\frac{5}{2} \\ -\frac{9}{19} & \frac{29}{5} & -\frac{45}{2} \\ -\frac{27}{19} & \frac{9}{5} & -\frac{41}{18} \end{pmatrix}$	A18

TABLE XI. The two-loop Yukawa contributions to the gauge sector β functions in Eq. (20) are detailed. The index p in y_{pk} labels the gauge groups while k refers to flavor. In addition to the Higgs bidoublet from the 10-dimensional representation (whose components are denoted according to the relevant gauge symmetry by h and ϕ) extra bidoublet components in $\overline{126}_H$ (denoted by H and Φ) survives from unification down to the Pati-Salam breaking scale as required by a realistic SM fermionic spectrum. The T_a factors are the generators of $SU(4)_C$ in the standard normalization. As a consequence of minimal fine-tuning, only one linear combination of 10_H and $\overline{126}_H$ doublets survives below the $SU(4)_C$ scale. The $U(1)_{R,X}$ mixing in the case $2_L 1_R 1_X 3_c$ is explicitly displayed.

G_p	y_{pk}	k	Gauge structure	Higgs representation	Tensor Δ	$\mathrm{Tr}[\Delta\Delta^\dagger]$
1_Y 2_L 3_c	$\begin{pmatrix} \frac{17}{10} & \frac{1}{2} & \frac{3}{2} \\ \frac{3}{2} & \frac{3}{2} & \frac{1}{2} \\ 2 & 2 & 0 \end{pmatrix}$	U D E	$\bar{Q}_{L_{kj}} U_R^i \tilde{h}_l$ $\bar{Q}_{L_{kj}} D_R^i h^l$ $\bar{L}_{L_k} E_R^i h^l$	h^l: $(+\frac{1}{2}, 2, 1)$	$\epsilon^{kl}\delta_{3i}{}^{j}$ $\delta_{2l}{}^{k}\delta_{3i}{}^{j}$ $\delta_{2l}{}^{k}$	6 6 2
2_L 1_{RR} 1_{RX} 1_{XR} 1_{XX} 3_c	$\begin{pmatrix} \frac{3}{2} & \frac{3}{2} & \frac{1}{2} & \frac{1}{2} \\ \frac{3}{2} & \frac{3}{2} & \frac{1}{2} & \frac{1}{2} \\ \frac{1}{2}\sqrt{\frac{3}{2}} & -\frac{1}{2}\sqrt{\frac{3}{2}} & -\frac{1}{2}\sqrt{\frac{3}{2}} & \frac{1}{2}\sqrt{\frac{3}{2}} \\ \frac{1}{2}\sqrt{\frac{3}{2}} & -\frac{1}{2}\sqrt{\frac{3}{2}} & -\frac{1}{2}\sqrt{\frac{3}{2}} & \frac{1}{2}\sqrt{\frac{3}{2}} \\ \frac{1}{2} & \frac{1}{2} & \frac{3}{2} & \frac{3}{2} \\ 2 & 2 & 0 & 0 \end{pmatrix}$	U D N E	$\bar{Q}_{L_{kj}} U_R^i \tilde{h}_l$ $\bar{Q}_{L_{kj}} D_R^i h^l$ $\bar{L}_{L_k} N_R \tilde{h}_l$ $\bar{L}_{L_k} E_R h^l$	h^l: $(2, +\frac{1}{2}, 0, 1)$	$\epsilon^{kl}\delta_{3i}{}^{j}$ $\delta_{2l}{}^{k}\delta_{3i}{}^{j}$ ϵ^{kl} $\delta_{2l}{}^{k}$	6 6 2 2
2_L 2_R 1_X 3_c	$\begin{pmatrix} 3 & 1 \\ 3 & 1 \\ 1 & 3 \\ 4 & 0 \end{pmatrix}$	Q L	$Q_L^{ik} Q_{Lj}^{cm} \phi^{ln}$ $L_L^k L_L^{cm} \phi^{ln}$	ϕ^{ln}: $(2, 2, 0, 1)$	$\epsilon_{kl}\epsilon_{mn}\delta_{3i}{}^{j}$ $\epsilon_{kl}\epsilon_{mn}$	12 4
2_L 1_X 4_C	$\begin{pmatrix} 2 & 2 \\ 2 & 2 \\ 2 & 2 \end{pmatrix}$	F^U F^D	$\bar{F}_{L_{kj}} F_R^{Ui} \tilde{h}_l$ $\bar{F}_{L_{kj}} F_R^{Di} h^l$	h^l: $(2, +\frac{1}{2}, 1)$	$\epsilon^{kl}\delta_{4i}{}^{j}$ $\delta_{2l}{}^{k}\delta_{4i}{}^{j}$	8 8
2_L 2_R 4_C	$\begin{pmatrix} 4 \\ 4 \\ 4 \end{pmatrix}$	F	$F_L^{ik} F_{Lj}^{cm} \phi^{ln}$	ϕ^{ln}: $(2, 2, 1)$	$\epsilon_{kl}\epsilon_{mn}\delta_{4i}{}^{j}$	16
2_L 1_X 4_C	$\begin{pmatrix} \frac{15}{4} & \frac{15}{4} \\ \frac{15}{4} & \frac{15}{4} \\ \frac{15}{4} & \frac{15}{4} \end{pmatrix}$	F^U F^D	$\bar{F}_{L_{kj}} F_R^{Ui} \tilde{H}_l^a$ $\bar{F}_{L_{kj}} F_R^{Di} H^{la}$	H^{la}: $(2, +\frac{1}{2}, 15)$	$\epsilon^{kl}(T_a)_i^j$ $\delta_l^k (T_a)_i^j$	15 15
2_L 2_R 4_C	$\begin{pmatrix} \frac{15}{2} \\ \frac{15}{2} \\ \frac{15}{2} \end{pmatrix}$	F	$F_L^{ik} F_{Lj}^{cm} \Phi^{lna}$	Φ^{lna}: $(2, 2, 15)$	$\epsilon_{kl}\epsilon_{mn}(T_a)_i^j$	30

analysis. The calculation of the $U(1)$ mixing coefficients and of the Yukawa contributions to the gauge coupling renormalization is detailed in Appendices A 1 and A 2, respectively.

1. Beta functions with $U(1)$ mixing

The basic building blocks of the one- and two-loop β functions for the Abelian couplings with $U(1)$ mixing, cf. Eqs. (14) and (15), can be conveniently written as

$$g_{ka} g_{kb} = g_{sa} \Gamma^{(1)}_{sr} g_{rb} \tag{A1}$$

and

$$g_{ka} g_{kb} g^2_{kc} = g_{sa} \Gamma^{(2)}_{sr} g_{rb}, \tag{A2}$$

where $\Gamma^{(1)}$ and $\Gamma^{(2)}$ are functions of the Abelian charges Q^a_k and, at two loops, also of the gauge couplings. In the case of interest, i.e. for two Abelian charges $U(1)_A$ and $U(1)_B$, one obtains

$$\Gamma^{(1)}_{AA} = (Q^A_k)^2, \qquad \Gamma^{(1)}_{AB} = \Gamma^{(1)}_{BA} = Q^A_k Q^B_k, \qquad \Gamma^{(1)}_{BB} = (Q^B_k)^2, \tag{A3}$$

and

$$\begin{aligned}
\Gamma^{(2)}_{AA} &= (Q^A_k)^4 (g^2_{AA} + g^2_{AB}) + 2(Q^A_k)^3 Q^B_k (g_{AA} g_{BA} + g_{AB} g_{BB}) \\
&\quad + (Q^A_k)^2 (Q^B_k)^2 (g^2_{BA} + g^2_{BB}), \\
\Gamma^{(2)}_{AB} &= \Gamma^{(2)}_{BA} = (Q^A_k)^3 Q^B_k (g^2_{AA} + g^2_{AB}) + 2(Q^A_k)^2 (Q^B_k)^2 \\
&\quad \times (g_{AA} g_{BA} + g_{AB} g_{BB}) + Q^A_k (Q^B_k)^3 (g^2_{BA} + g^2_{BB}), \\
\Gamma^{(2)}_{BB} &= (Q^A_k)^2 (Q^B_k)^2 (g^2_{AA} + g^2_{AB}) + 2 Q^A_k (Q^B_k)^3 \\
&\quad \times (g_{AA} g_{BA} + g_{AB} g_{BB}) + (Q^B_k)^4 (g^2_{BA} + g^2_{BB}).
\end{aligned} \tag{A4}$$

All other contributions in Eqs. (14) and (15) can be easily obtained from Eqs. (A3) and (A4) by including the appropriate group factors. It is worth mentioning that for complete $SO(10)$ multiplets, $(Q^A_k)^n (Q^B_k)^m = 0$ for n and m

odd (with $n + m = 2$ at one loop and $n + m = 4$ at the two-loop level).

By evaluating Eqs. (A3) and (A4) for the particle content relevant to the $2_L 1_R 1_X 3_c$ stages in chains VIII–XII, and by substituting into Eqs. (14) and (15), one finally obtains

(i) Chains VIII–XII with $\overline{126}_H$ in the Higgs sector:

$$\begin{aligned}
\gamma_{RR} &= \frac{9}{2} + \frac{1}{(4\pi)^2}\left[\frac{15}{2}(g_{RR}^2 + g_{RX}^2) - 4\sqrt{6}(g_{RR}g_{XR} + g_{RX}g_{XX}) + \frac{15}{2}(g_{XR}^2 + g_{XX}^2) + \frac{3}{2}g_L^2 + 12g_c^2\right],\\
\gamma_{RX} &= \gamma_{XR} = -\frac{1}{\sqrt{6}} + \frac{1}{(4\pi)^2}[-2\sqrt{6}(g_{RR}^2 + g_{RX}^2) + 15(g_{RR}g_{XR} + g_{RX}g_{XX}) - 3\sqrt{6}(g_{XR}^2 + g_{XX}^2)],\\
\gamma_{XX} &= \frac{9}{2} + \frac{1}{(4\pi)^2}\left[\frac{15}{2}(g_{RR}^2 + g_{RX}^2) - 6\sqrt{6}(g_{RR}g_{XR} + g_{RX}g_{XX}) + \frac{25}{2}(g_{XR}^2 + g_{XX}^2) + \frac{9}{2}g_L^2 + 4g_c^2\right],\\
\gamma_L &= -\frac{19}{6} + \frac{1}{(4\pi)^2}\left[\frac{1}{2}(g_{RR}^2 + g_{RX}^2) + \frac{3}{2}(g_{XR}^2 + g_{XX}^2) + \frac{35}{6}g_L^2 + 12g_c^2\right],\\
\gamma_c &= -7 + \frac{1}{(4\pi)^2}\left[\frac{3}{2}(g_{RR}^2 + g_{RX}^2) + \frac{1}{2}(g_{XR}^2 + g_{XX}^2) + \frac{9}{2}g_L^2 - 26g_c^2\right];
\end{aligned} \tag{A5}$$

(ii) Chains VIII–XII with $\overline{16}_H$ in the Higgs sector:

$$\begin{aligned}
\gamma_{RR} &= \frac{17}{4} + \frac{1}{(4\pi)^2}\left[\frac{15}{4}(g_{RR}^2 + g_{RX}^2) - \frac{1}{2}\sqrt{\frac{3}{2}}(g_{RR}g_{XR} + g_{RX}g_{XX}) + \frac{15}{8}(g_{XR}^2 + g_{XX}^2) + \frac{3}{2}g_L^2 + 12g_c^2\right],\\
\gamma_{RX} &= \gamma_{XR} = -\frac{1}{4\sqrt{6}} + \frac{1}{(4\pi)^2}\left[-\frac{1}{4}\sqrt{\frac{3}{2}}(g_{RR}^2 + g_{RX}^2) + \frac{15}{4}(g_{RR}g_{XR} + g_{RX}g_{XX}) - \frac{3}{8}\sqrt{\frac{3}{2}}(g_{XR}^2 + g_{XX}^2)\right],\\
\gamma_{XX} &= \frac{33}{8} + \frac{1}{(4\pi)^2}\left[\frac{15}{8}(g_{RR}^2 + g_{RX}^2) - \frac{3}{4}\sqrt{\frac{3}{2}}(g_{RR}g_{XR} + g_{RX}g_{XX}) + \frac{65}{16}(g_{XR}^2 + g_{XX}^2) + \frac{9}{2}g_L^2 + 4g_c^2\right],\\
\gamma_L &= -\frac{19}{6} + \frac{1}{(4\pi)^2}\left[\frac{1}{2}(g_{RR}^2 + g_{RX}^2) + \frac{3}{2}(g_{XR}^2 + g_{XX}^2) + \frac{35}{6}g_L^2 + 12g_c^2\right],\\
\gamma_c &= -7 + \frac{1}{(4\pi)^2}\left[\frac{3}{2}(g_{RR}^2 + g_{RX}^2) + \frac{1}{2}(g_{XR}^2 + g_{XX}^2) + \frac{9}{2}g_L^2 - 26g_c^2\right].
\end{aligned} \tag{A6}$$

By setting $\gamma_{XR} = \gamma_{RX} = 0$ and $g_{XR} = g_{RX} = 0$ in Eqs. (A5) and (A6) one obtains the one- and two-loop β coefficients in the diagonal approximation, as reported in Table VII. The latter are used in Figs. 1 and 2 for the only purpose of exhibiting the effect of the Abelian mixing in the gauge coupling renormalization.

2. Yukawa contributions

The Yukawa couplings enter the gauge β functions first at the two-loop level, cf. Eqs. (3) and (14). Since the notation adopted in Eqs. (6) and (7) is rather concise we shall detail the structure of Eq. (6), paying particular attention to the calculation of the y_{pk} coefficients in Eq. (20).

The trace on the RHS of Eq. (6) is taken over all indices of the fields entering the Yukawa interaction in Eq. (7). Considering, for instance, the up-quark Yukawa sector of the SM the term $\bar{Q}_L Y_U U_R \tilde{h}$ + H.c. (with $\tilde{h} = i\sigma_2 h^*$) can be explicitly written as

$$Y_U^{ab}\varepsilon^{kl}\delta_{3j}{}^{i}\bar{Q}_{Lik}^{a}U_R^{bj}h_l^* + \text{H.c.}, \tag{A7}$$

where $\{a, b\}$, $\{i, j\}$, and $\{k, l\}$ label flavor, $SU(3)_c$ and $SU(2)_L$ indices, respectively, while δ_n denotes the n-dimensional Kronecker δ symbol. Thus, the Yukawa coupling entering Eq. (6) is a six-dimensional object with the index structure $Y_U^{ab}\varepsilon^{kl}\delta_{3j}^{i}$. The contribution of Eq. (A7) to the three y_{pU} coefficients (conveniently separated into two terms corresponding to the fermionic representations Q_L and U_R) can then be written as

$$\begin{aligned}
y_{pU} = \frac{1}{d(G_p)}&[C_2^{(p)}(Q_L)\\
&+ C_2^{(p)}(U_R)]\sum_{ab,ij,kl} Y_U^{ab}\varepsilon^{kl}\delta_{3j}{}^{i}Y_U^{ab*}\varepsilon_{kl}\delta_{3i}{}^{j}.
\end{aligned} \tag{A8}$$

The sum can be factorized into the flavor space part

$\sum_{ab} Y_U^{ab*} Y_U^{ab} = \mathrm{Tr}[Y_U Y_U^\dagger]$ times the trace over the gauge contractions $\mathrm{Tr}[\Delta\Delta^\dagger]$ where $\Delta \equiv \varepsilon^{kl}\delta_{3j}{}^{i}$. For the SM gauge group (with the properly normalized hypercharge) one then obtains $y_{1U} = \frac{17}{10}$, $y_{2U} = \frac{3}{2}$ and $y_{3U} = 2$, that coincide with the values given in the first column of the matrix (B.5) in Ref. [21].

All of the y_{pk} coefficients as well as the structures of the relevant Δ tensors are reported in Table XI.

[1] H. Georgi, in *Particles and Fields*, edited by C. E. Carlson (AIP, New York, 1975); H. Fritzsch and P. Minkowski, Ann. Phys. (N.Y.) **93**, 193 (1975).

[2] P. Minkowski, Phys. Lett. B **67**, 421 (1977); M. Gell-Mann, P. Ramond, and R. Slansky, in *Supergravity*, edited by P. van Nieuwenhuizen and D. Z. Freedman (North-Holland, Amsterdam, 1979), p. 315; T. Yanagida, in *Proceedings of the Workshop on the Baryon Number of the Universe and Unified Theories*, edited by O. Sawada and A. Sugamoto (KEK, Tsukuba, Japan, 1979), p. 95; S. L. Glashow, Report No. HUTP-79-A059, 1979, p. 687; R. N. Mohapatra and G. Senjanović, Phys. Rev. Lett. **44**, 912 (1980).

[3] M. Magg and C. Wetterich, Phys. Lett. B **94**, 61 (1980); J. Schechter and J. W. F. Valle, Phys. Rev. D **22**, 2227 (1980); G. Lazarides, Q. Shafi, and C. Wetterich, Nucl. Phys. **B181**, 287 (1981); R. N. Mohapatra and G. Senjanović, Phys. Rev. D **23**, 165 (1981).

[4] C. S. Aulakh, B. Bajc, A. Melfo, A. Rasin, and G. Senjanovic, Nucl. Phys. **B597**, 89 (2001); T. Fukuyama and N. Okada, J. High Energy Phys. 11 (2002) 011; B. Bajc, G. Senjanovic, and F. Vissani, Phys. Rev. Lett. **90**, 051802 (2003); H. S. Goh, R. N. Mohapatra, and S. P. Ng, Phys. Lett. B **570**, 215 (2003); T. Fukuyama, T. Kikuchi, and N. Okada, Phys. Rev. D **68**, 033012 (2003); C. S. Aulakh, B. Bajc, A. Melfo, G. Senjanovic, and F. Vissani, Phys. Lett. B **588**, 196 (2004); H. S. Goh, R. N. Mohapatra, and S. P. Ng, Phys. Rev. D **68**, 115008 (2003); T. Fukuyama, A. Ilakovac, T. Kikuchi, S. Meljanac, and N. Okada, Eur. Phys. J. C **42**, 191 (2005); B. Bajc, A. Melfo, G. Senjanovic, and F. Vissani, Phys. Rev. D **70**, 035007 (2004); B. Bajc, G. Senjanovic, and F. Vissani, Phys. Rev. D **70**, 093002 (2004); B. Dutta, Y. Mimura, and R. N. Mohapatra, Phys. Rev. D **69**, 115014 (2004); H. S. Goh, R. N. Mohapatra, and S. Nasri, Phys. Rev. D **70**, 075022 (2004); C. S. Aulakh and A. Girdhar, Int. J. Mod. Phys. A **20**, 865 (2005); C. S. Aulakh and A. Girdhar, Nucl. Phys. **B711**, 275 (2005); T. Fukuyama, A. Ilakovac, T. Kikuchi, S. Meljanac, and N. Okada, Phys. Rev. D **72**, 051701 (2005); C. S. Aulakh, Phys. Rev. D **72**, 051702 (2005); T. Fukuyama, T. Kikuchi, and T. Osaka, J. Cosmol. Astropart. Phys. 06 (2005) 005; S. Bertolini, M. Frigerio, and M. Malinsky, Phys. Rev. D **70**, 095002 (2004); S. Bertolini and M. Malinsky, Phys. Rev. D **72**, 055021 (2005); K. S. Babu and C. Macesanu, Phys. Rev. D **72**, 115003 (2005); B. Dutta, Y. Mimura, and R. N. Mohapatra, Phys. Rev. D **72**, 075009 (2005); B. Bajc, A. Melfo, G. Senjanovic, and F. Vissani, Phys. Lett. B **634**, 272 (2006); C. S. Aulakh, arXiv:hep-ph/0506291; C. S. Aulakh and S. K. Garg, Nucl. Phys. **B757**, 47 (2006); L. Lavoura, H. Kühböck, and W. Grimus, Nucl. Phys. **B754**, 1 (2006); R. N. Mohapatra and A. Y. Smirnov, Annu. Rev. Nucl. Part. Sci. **56**, 569 (2006); S. Bertolini, T. Schwetz, and M. Malinsky, Phys. Rev. D **73**, 115012 (2006); W. Grimus and H. Kuhbock, Eur. Phys. J. C **51**, 721 (2007); C. S. Aulakh, Phys. Lett. B **661**, 196 (2008); B. Bajc, I. Dorsner, and M. Nemevsek, J. High Energy Phys. 11 (2008) 007.

[5] B. Bajc, A. Melfo, G. Senjanovic, and F. Vissani, Phys. Rev. D **73**, 055001 (2006).

[6] J. M. Gipson and R. E. Marshak, Phys. Rev. D **31**, 1705 (1985).

[7] D. Chang, R. N. Mohapatra, J. Gipson, R. E. Marshak, and M. K. Parida, Phys. Rev. D **31**, 1718 (1985).

[8] N. G. Deshpande, E. Keith, and P. B. Pal, Phys. Rev. D **46**, 2261 (1992).

[9] N. G. Deshpande, E. Keith, and P. B. Pal, Phys. Rev. D **47**, 2892 (1993).

[10] V. V. Dixit and M. Sher, Phys. Rev. D **40**, 3765 (1989).

[11] R. N. Mohapatra and M. K. Parida, Phys. Rev. D **47**, 264 (1993).

[12] L. Lavoura and L. Wolfenstein, Phys. Rev. D **48**, 264 (1993).

[13] D. Chang, R. N. Mohapatra, and M. K. Parida, Phys. Rev. Lett. **52**, 1072 (1984); D. Chang, R. N. Mohapatra, and M. K. Parida, Phys. Rev. D **30**, 1052 (1984).

[14] V. A. Kuzmin and M. E. Shaposhnikov, Phys. Lett. B **92**, 115 (1980).

[15] T. W. B. Kibble, G. Lazarides, and Q. Shafi, Phys. Rev. D **26**, 435 (1982).

[16] F. del Aguila and L. E. Ibanez, Nucl. Phys. **B177**, 60 (1981).

[17] R. N. Mohapatra and G. Senjanovic, Phys. Rev. D **27**, 1601 (1983).

[18] D. R. T. Jones, Nucl. Phys. **B75**, 531 (1974).

[19] W. E. Caswell, Phys. Rev. Lett. **33**, 244 (1974).

[20] D. R. T. Jones, Phys. Rev. D **25**, 581 (1982).

[21] M. E. Machacek and M. T. Vaughn, Nucl. Phys. **B222**, 83 (1983); M. E. Machacek and M. T. Vaughn, Nucl. Phys. **B236**, 221 (1984); M. E. Machacek and M. T. Vaughn, Nucl. Phys. **B249**, 70 (1985).

[22] B. Holdom, Phys. Lett. B **166**, 196 (1986).

[23] M. x. Luo and Y. Xiao, Phys. Lett. B **555**, 279 (2003).

[24] F. del Aguila, G. D. Coughlan, and M. Quiros, Nucl. Phys. **B307**, 633 (1988); F. del Aguila, G. D. Coughlan, and M. Quiros, Nucl. Phys. **B312**, 751(E) (1989).

[25] F. del Aguila, M. Masip, and M. Perez-Victoria, Nucl. Phys. **B456**, 531 (1995).

[26] S. Weinberg, Phys. Lett. B **91**, 51 (1980).

[27] L. J. Hall, Nucl. Phys. **B178**, 75 (1981).

[28] C. Amsler *et al.* (Particle Data Group), Phys. Lett. B **667**, 1 (2008).
[29] L. Lavoura, Phys. Rev. D **48**, 2356 (1993).
[30] C. S. Aulakh and R. N. Mohapatra, Phys. Rev. D **28**, 217 (1983).
[31] R. N. Mohapatra, arXiv:0902.0834.
[32] M. Yasue, Phys. Rev. D **24**, 1005 (1981).
[33] J. A. Harvey, D. B. Reiss, and P. Ramond, Nucl. Phys. **B199**, 223 (1982).
[34] G. Anastaze, J. P. Derendinger, and F. Buccella, Z. Phys. C **20**, 269 (1983).
[35] K. S. Babu and E. Ma, Phys. Rev. D **31**, 2316 (1985).
[36] M. Abud, F. Buccella, L. Rosa, and A. Sciarrino, Z. Phys. C **44**, 589 (1989); F. Acampora, G. Amelino-Camelia, F. Buccella, O. Pisanti, L. Rosa, and T. Tuzi, Nuovo Cimento Soc. Ital. Fis. A **108**, 375 (1995).